

Northern hemispheric atmospheric ethane trends (2006-2016) with reference to methane and propane ~~Global atmospheric ethane, propane and methane trends (2006-2016)~~

5

Mengze Li ^{1,2}, Andrea Pozzer ¹, Jos Lelieveld ^{1,3}, Jonathan Williams ^{1,3}

1 Max Planck Institute for Chemistry, Hahn-Meitner-Weg 1, 55128 Mainz, Germany

2 Now at: Department of Climate and Space Sciences and Engineering, University of Michigan, Ann Arbor, USA

3 Climate and Atmosphere Research Center, The Cyprus Institute, 1645, Nicosia, Cyprus

10 *Correspondence to:* Jonathan Williams (jonathan.williams@mpic.de); Andrea Pozzer (andrea.pozzer@mpic.de); Mengze Li (mengze.li@mpic.de)

Abstract. Methane, ethane, and propane are among the most abundant hydrocarbons in the atmosphere. These compounds have many emission sources in common and are all primarily removed through OH oxidation. Their mixing ratios and long-term trends in the upper troposphere and stratosphere are rarely reported due to the paucity of measurements. In this study, we present long-term (2006-2016) ~~northern hemispheric~~ ethane, propane, and methane data from airborne observation in the Upper Troposphere - Lower Stratosphere (UTLS) region ~~from IAGOS-CARIBIC project~~, combined with atmospheric model (EMAC) simulations for ethane at the same times and locations, ~~to focus on global ethane trends. The model simulations, and methane and propane observations provide additional information for understanding northern hemispheric ethane trends and emissions, which is the major focus of this study.~~ The model uses the Copernicus emission inventory CAMS-GLOB and distinguishes 132 ethane emission sectors (natural and anthropogenic): BIO (biogenic emission), BIB (biomass burning), AWB (agricultural waste burning), ENE (power generation), FEF (fugitives), IND (industrial processes), RES (residential energy use), SHP (ships), SLV (solvents), SWD (solid waste and waste-water), TNR (off-road transportation), ~~and~~ TRO (road transportation), ~~and~~ AIR (aviation). The results from the model simulations were compared with observational data and further optimized. The Northern Hemispheric (NH) upper tropospheric and stratospheric ethane trends were 0.33 ± 0.27 (mean \pm one standard deviation) %/yr and -3.6 ± 0.3 %/yr, respectively, in 2006-2016. The global ethane emission for this decade was estimated to be 19.328 Tg/yr. Trends of methane and propane, and of the 132 model sectors provided more insights on the variation of ethane trends. FEF, RES, TRO, SWD, and BIB are the top five contributing sectors to the observed ethane trends. An ethane plume for NH upper troposphere and stratosphere in 2010-2011 was identified to be due to fossil ~~fuel-fuel~~-related emissions, likely from oil and gas exploitation. The discrepancy between model results and observations suggests that the current ~~ethane emission~~-inventories have underestimated ethane emission and must be improved and higher temporal-spatial resolution data of ethane are

needed. This dataset is of value to future global ethane budget estimates and the optimization of current ethane
35 inventories. The data are publicly accessible at <https://doi.org/10.5281/zenodo.5112059> [6301729](https://doi.org/10.5281/zenodo.6301729) (Li et al., 2021).

1. Introduction

Ethane (C₂H₆) is among the most abundant non-methane hydrocarbons (NMHC) present in the atmosphere. Major sources of ethane to the atmosphere are via natural gas and oil production (~62%), biofuel combustion (20%), and biomass burning (18%). Interestingly, 84% of its total emissions are from the Northern Hemisphere (NH) (Xiao et al., 2008). Oxidation by hydroxyl (OH) radicals is the major atmospheric loss process for tropospheric ethane, while in the stratosphere the reaction with chlorine (Cl) radicals provides an additional loss processes (Li et al., 2018). Due to the seasonal variation of ethane emissions and the photochemically generated OH radicals, ethane has a clear annual cycle in concentrationmole fractions, showing higher levels in winter. Its global lifetime is circa three months, with a minimum in summer (~2 months) and a maximum in winter (~10 months) (Xiao et al., 2008; Helmig et al., 2016; Li et al., 2018). Ethane oxidation forms acetaldehyde, which in turn contributes to the formation of PAN (peroxyacetyl nitrate) or peracetic acid depending on the levels of NO_x (Millet et al., 2010). PAN acts as a reservoir species of nitrogen oxides (NO_x) and can strongly affect tropospheric ozone distributions by transporting NO_x from the point of emission to remote locations. Furthermore, PAN is known to be a secondary pollutant like ozone with negative impacts on regional air quality and human health (Rudolph, 1995; González Abad et al., 2011; Fischer et al., 2014; Monks et al., 2018; Kort et al., 2016; Tzompa-Sosa et al., 2017; Dalsøren et al., 2018; Pozzer et al., 2020).

Several recent studies have estimated global ethane budgets using a combination of observations and model simulations. Xiao et al. (2008) estimated a global ethane source of 13.0 Tg/yr based on methane emissions for the 1990s. This study included information on sectoral and geographical ethane emissions, although the inventory might partially be outdated, at least for North America, due to the changes in oil and gas extraction since 2004 (Tzompa-Sosa et al., 2017). Simpson et al. (2012) reported a total 21% decrease in global ethane emissions from 14.3 to 11.3 Tg/yr from 1984 to 2010, likely due to the decline in fugitive emissions from fossil fuel extraction and use. Monks et al. (2018) estimated the global ethane emission in 2008 to be 15.4 ± 2.3 Tg/yr. Hausmann et al. (2016) calculated the contribution from oil and natural gas to the total ethane emission increase of 1-11 Tg/yr over 2007-2014. Franco et al. (2016) reported a global ethane emission of 18.2 Tg/yr for 2014 and that North American anthropogenic ethane emissions increased by 75% over 2008-2014. Helmig et al. (2016) calculated a growth rate of 0.42 (± 0.19) Tg/yr of NH ethane emission

between mid-2009 and mid-2014, and Pozzer et al. (2020) estimated a 2.1 Tg/yr increase of global anthropogenic ethane from 13.2 to 15.3 Tg/yr over the same period.

Despite the general agreement in global emission estimates, multiple studies have pointed out that the current inventories used in atmospheric chemistry models underestimate ethane emissions by up to a factor of 2-3 (Tzompa-Sosa et al., 2017; Angot et al., 2021; Monks et al., 2018; Dalsøren et al., 2018; Franco et al., 2016; Pétron et al., 2014; Tilmes et al., 2016; Emmons et al., 2015). Dalsøren et al. (2018) concluded that the major source of uncertainty in these inventories comes from the assumed speciation of NMVOCs (non-methane volatile organic compounds) and disaggregation of carbon emissions into individual species based on little available data. Therefore, ~~in order~~ to determine the global ethane trends in terms of mole fractions and emissions with greater certainty, long-term global ethane datasets from observations and model simulations with minimal ~~local~~ influences from local sources (e.g. observations at higher altitudes) are required (Angot et al., 2021; Gardiner et al., 2008).

Previous studies attempting to understand the distribution, emissions, lifetime, and atmospheric trends of ethane have tended to be from surface sites, either from a regionally focused intensive field measurement campaign (e.g. Kort et al. (2016)) or from networks of remote sampling stations (e.g. Franco et al. (2015), Helmig et al. (2016)). The advantage of surface sites is that they are easily accessed and maintained, however, such measurements inevitably reflect the local or regional situation, and changes in emissions immediately upwind of a measurement location can affect the results, masking any underlying long-term global trend. In addition, most ethane measurement sites are located in developed countries, such as ~~in~~ North America and Europe, while ethane observations in the rest of the world are sparse. This too hinders the assessment of global ethane trends, for while one country's emission may be declining another's could be increasing rapidly. For the aforementioned reasons, it is advantageous to assess the global long-term ethane trend from the upper troposphere and even the stratosphere where emissions can be expected to be well mixed by atmospheric circulations. In particular, the trend of ethane in the more isolated and remote stratosphere is of interest when assessing long-term changes.

In this study, we use airborne observations covering the Northern Hemisphere (NH), including over regions where ground measurements are not set up or not possible. We present long-term northern hemispheric global and geographically delineated (North America, Asia, Europe) ethane

trends in the upper troposphere and stratosphere for the decade 2006-2016 derived using airborne measurements and global model simulations. In addition, the trends of methane and propane collected from the same observations are examined to better understand the observed variation of NH ethane trends, as they have common sources and sinks in the atmosphere. All the data used in this study are publicly available at <https://doi.org/10.5281/zenodo.51120596301729>. These data can be used for further analysis on global and regional trends, emissions and lifetime of methane, ethane, and propane, their contributions to climate change, stratosphere-troposphere exchange, and improvement of current inventories and atmospheric models.

2. Materials and Methods

2.1 IAGOS-CARIBIC observation

The IAGOS-CARIBIC project (In-service Aircraft for a Global Observing System-Civil Aircraft for the Regular Investigation of the atmosphere Based on an Instrument Container) is an ~~aircraft~~ aircraft-based scientific project with the aim of monitoring long-term global atmospheric physics and chemistry (Brenninkmeijer et al., 2007). The flight altitudes are at ~10 km, which is in the Upper Troposphere-Lower Stratosphere (UTLS) region. A ~~custom~~-custom-built whole air sampler collects pressurized air samples during each flight, and these samples are subsequently measured in the laboratory with Gas Chromatography (GC) coupled with three detectors: GC-ECD and GC-FID for greenhouse gas measurements (methane, carbon dioxide, nitrous oxide, and sulphur hexafluoride) (Schuck et al., 2009), and GC-FID and GC-AED for volatile organic compound measurements, including ethane and propane (Baker et al., 2010; Karu et al., 2021). The precision of ethane and propane data used in this study is 0.2% and 0.8%, respectively (Baker et al., 2010), and of methane 0.17% (Schuck et al., 2009). Details regarding operational and analytical measurement procedures, calibration scales, and quality assurance are well documented in the cited references, and summarized as follows.

Each IAGOS-CARIBIC flight normally consists of four flight sequences with a total number of 116 air samples collected by whole air samplers (flasks). The inlet and outlet of each flask are connected by multi-position valves which can be automatically switched with programming. A

125 pumping system and pressure sensors are connected to the inlet valves to guarantee the final pressure in each flask to be around 4.5 bar. The outlet valves are connected to ambient air. Prior to pressurization, each flask is flushed with ambient air for 10 times (about 5-10 min). The average filling (sampling) time of each flask is about 45s (range 0.5-1.5 min) depending on the flight altitude, resulting a spatial resolution of 7-21km.

130 Methane, ethane, and propane were measured with a HP 6890 GC with a polymer Porapak Q 3/4" column (10 ft, 100/120 mesh) installed in a single oven. Nitrogen (N₂, purity 99.999%) was used as carrier gas at a constant flow rate of 50ml/min. The GC was operated at oven temperature of 220°C with flow rates of synthetic air of 250ml/min and hydrogen of 80ml/min. Water vapor in samples was removed by passing through a drying tube at the start of the analysis. The calibration standards and reference gas cylinders were ordered from NOAA (for methane), and the National
135 Physical Laboratory (for ethane and propane) which are certified against World Meteorological Organization (WMO) Global Atmosphere Watch (GAW) program scale, and they are regularly renewed within every three years which warrants the stability of calibration gases. Three injections of calibration standards were made in between samples of each flight sequence in order to maintain the quality of measurements and reduce uncertainty.

140 The upper tropospheric and stratospheric air samples were differentiated by using potential vorticity (hereafter PV, unit PVU). Northern hemispheric air samples with PV larger than 2 PVU were identified as stratospheric samples, otherwise as upper tropospheric samples. Figure 1 shows the geographical distributions of upper tropospheric and stratospheric samples, and spatial segregation. It is noted that the region designated must not correspond to the source region, only
145 the geographical location of the data points.

2.2 EMAC global model

The ECHAM/MESSy Atmospheric Chemistry (EMAC) model is a numerical chemistry and climate simulation system that includes sub-models describing tropospheric and middle atmosphere processes and their interaction with oceans, land, and human influences (Jöckel et al.,
150 2010). It uses the second version of the Modular Earth Submodel System (MESSy2) to link multi-institutional computer codes. The core atmospheric model is the 5th generation European Centre Hamburg general circulation model (ECHAM5, Roeckner et al. (2006)). For the present study, we

applied EMAC (ECHAM5 version 5.3.02, MESSy version 2.55.0) in the T63L47MA-resolution, i.e. with a spherical truncation of T63 (corresponding to a quadratic Gaussian grid of approx. 1.8 by 1.8 degrees in latitude and longitude) with 47 vertical hybrid pressure levels up to 0.01 hPa (~80 km). The model has been weakly nudged towards the ERA5 reanalysis data of the ECMWF (Hersbach et al., 2020). The chemical mechanism comprises methane, alkanes, and alkenes up to C₄, ozone, odd nitrogen, some selected non-methane hydrocarbons (NMHCs), heterogeneous reactions, etc. In total, 310 reactions of 155 species are included in the model. The photolysis rates are calculated following Sander et al. (2014). No chlorine chemistry is included in the model. To account for realistic emissions, the CAMS-GLOB-ANT v4.2 emission inventory data is used for model simulations (Granier et al., 2019; Guevara et al., 2020). In this study, we have included 13 emission sectors (shown in Table 1) which are BIO (biogenic emission), BIB (biomass burning), AWB (agricultural waste burning), ENE (power generation), FEF (fugitives), IND (industrial processes), RES (residential energy use), SHP (ships), SLV (solvents), SWD (solid waste and waste water), TNR (off-road transportation), TRO (road transportation), and AIR (aviation). It is noted that AIR, BIB and BIO were combined as one sector to reduce the uncertainty. AIR is not shown in Table 1 as its contribution is negligible.

It has been shown by multiple studies that the ethane emissions due to fossil fuel combustion are strongly underestimated in the emissions database (Guevara et al., 2021; Pozzer et al., 2020; Helmig et al., 2016). In this work, we therefore increased the anthropogenic emissions of ethane of a factor of 2.47 to match (for the year 2010) the total amount suggested by Pozzer et al. (2020) although ~~theis~~ value used in this study (~11.8 Tg/yr) slightly underestimates the measured concentrationmole fraction as shown in Pozzer et al. (2020) (13.2 Tg/yr). ~~In the later sections of this paper, We~~ further optimized modeled ethane mole fractions for each emission sector (referred to as “opt” in the later figures and “optimized” in the later texts). The model optimization is done by increasing the emissions of each input emission sector by 45%. We found that the root mean squared error (RMSE) between the modeled and observational ethane mole fractions for the whole dataset was theat a minimum after aby 45% increase in the input emissions. increased the total emission by 45% to match the airborne observation data, and Tthe input estimated ethane emissions from natural and anthropogenic sources are presented in Table 1, together with a description for each sector and optimized sectoral emissions (will be discussed in the *Results and Discussion* section).

In this study, two types of ethane trends were presented with the model simulation: (1) constant meteorology and constant emission (hereafter called climatology), sampled at the IAGOS-CARIBIC sampling location with S4D algorithm (sampling in 4 dimensions) described in Jöckel et al. (2010). Any trends (or changes) detected in this simulation would be caused by differences in sample location and timing. (2) real meteorological conditions from ECMWF and the adjusted emissions described above, sampled at the IAGOS-CARIBIC sampling location with S4D algorithm (Jöckel et al., 2010).

2.3 Trend analysis

The trend and seasonality analysis algorithm (“Prophet”) used in this study has been described in detail elsewhere (Taylor and Letham, 2018). The “Prophet” algorithm has been shown to perform well with non-continuous ~~time-time~~-series datasets (Li et al., 2022), as is the case for ~~the~~-aircraft data. The trend analysis model has four components: trend (non-periodic changes), seasonality (periodic changes), holiday effects, and error (idiosyncratic changes). In this study, effects of holidays are not included. We used a linear model with change points for the trend component, and the trend function consists of growth rate, adjustments of growth rate, and offset parameter. The flexibility of trend (e.g. overfitting or underfitting) can be adjusted by the parameter “changepoint_prior_scale”. A change point represents the moments where the data shifts directions. The value of the parameter “changepoint_prior_scale” represents the strength of change points, more change points will be automatically detected when the value of this parameter increases. Seasonality is estimated by Fourier series (Harvey and Shephard, 1993). The uncertainty interval was set to be 95%. The code of trend analysis in Python for this study can be found in the Supplementary Material. Figure S1 shows the ethane trend and seasonality at Iceland estimated by “Prophet” algorithm. Compared with the trend and seasonality estimated by ~~the~~ NOAA algorithm (www.esrl.noaa.gov/gmd/ccgg/mb1/crvfit/crvfit.html) using the same dataset in Figure 1(b) of Helmig et al. (2016), the seasonality of ethane is well captured by both algorithms and the results match well with each other. The uncertainty from the trend analysis is estimated by applying ten fitting levels on the trend (i.e. “changepoint_prior_scale” = 0.1, 0.2, 0.3, ..., 0.9, 1.0). The difference between the most underfitting to most overfitting is taken as the uncertainty and the average value of the ten fitting levels is used to represent the underlying long-term trend.

215 In this study, we also calculated simple linear trends (hereafter as linear trend to distinguish with the trends derived from “Prophet” algorithm) within a time period as follows:

$$\text{Linear trend} = (C_{\text{End}} - C_{\text{Start}}) / (t_{\text{End}} - t_{\text{Start}}) \quad (1)$$

where t_{End} and t_{Start} represent the end and start date and time of the target time period, C_{End} or C_{Start} is the mole fraction of trace gases (ethane, methane or propane) at the end or start date and time.

220 3. Results and Discussion

3.1 Literature perspective of global ethane trends

Many studies have reported ethane trend analysis based on either ground-based sampling or FTIR (Fourier Transform Infrared Spectrometer) measurements. A summary of these studies is shown in Table 2. In the troposphere (Table 2(a)), the trends of C_2H_6 partial column at four European sites (Jungfraujoch, Zugspitze, Harestua and Kiruna) during 1996-2006 were between about -1.09 to -2.11%/yr (Angelbratt et al., 2011). Simpson et al. (2012) concluded a strong global ethane decline of 21% over 26 years (1984-2010), with a stronger decline occurring from 1984 to 1999 (-7.2 ± 1.7 ppt/yr) than from 2000 to 2010 (-1.9 ± 1.3 ppt/yr). Franco et al. (2015) showed the ethane trend at Jungfraujoch to be -0.92%/yr during 1994-2008, followed by a strong positive trend of 4.9%/yr during 2009-2014, which may be related to the growth of emissions from shale gas exploitation in North America. Helmig et al. (2016) calculated a mean ethane growth rate of 2.9-4.7%/yr from 2009 to 2014 at 32 NH ground measurement sites, and concluded that North American oil and gas development was the primary source of the increasing emission of ethane. Franco et al. (2016) compared the ethane total column change at six sites across NH for the period of 2003-2008 and 2009-2014, and also revealed a sharp increase of 3-5%/yr during 2009-2014 compared with 2003-2008, which was associated with oil and gas industry emission. They also specifically estimated a 1.2 Tg/yr increase of anthropogenic ethane emission from North America between 2008-2014. Hausmann et al. (2016) presented a positive ethane trend of ca. 4.6%/yr at Zugspitze (47° N) and a negative trend of ca. -2.5%/yr at Lauder (45° S) for 2007-2014, and inferred an ethane increase from oil and gas emission of 1-11 Tg/yr for 2007-2014. Angot et al. (2021) showed an increase in ethane trend of ca. 5.6%/yr at GEOSummit (73°N) for 2010-2014, followed by a temporary pause

of ethane growth in 2015-2018. Sun et al. (2021) presented a negative ethane trend of $-2.6 \pm 1.3\%/yr$ over 2015-2020 in a densely populated eastern Chinese city Hefei. In this study, we estimated an increasing NH upper tropospheric ethane trend of $0.33 \pm 0.27\%/yr$ (mean \pm 1SD) between February 2006 and February 2016 (relative to February 2006, thereafter same).

In contrast to tropospheric ethane trends, trends in the stratosphere have been far less investigated. Gardiner et al. (2008) (Table 2 (b)) presented annual trend in stratospheric ethane column (relative to year 2000) at six sites and these varied from 0.43 to $-3.31\%/yr$ until the year 2005. Franco et al. (2015) reported ethane trends at 8-16 km measured at Jungfrauoch of $-1.75 \pm 1.30\%/yr$ (for 2004-2008) and $9.4 \pm 3.2\%/yr$ (for 2009-2013), indicating an $\sim 11\%$ sharp increase since 2009. Helmig et al. (2016) showed that the UTLS column ethane (8-21km) measured at Jungfrauoch was decreasing at $-1.0 \pm 0.2\%/yr$ (1995-2009) and started a sharp increase at rate of $6.0 \pm 1.1\%/yr$ from 2009 until 2015, while the difference in trend growth rate between the two time periods is smaller for the mid-tropospheric column (3.6-8 km): $-0.8 \pm 0.3\%/yr$ (1995-2009) and $4.2 \pm 1.0\%/yr$ (2009-2015). In this study, we derived a NH lowermost stratospheric ethane decreasing trend of $-3.6 \pm 0.3\%/yr$ for the period February 2006 – February 2016.

It is noted that our aircraft samples have significantly different spatial distributions compared with the studies summarized above, any comparison should be made in a careful manner. When comparing surface and airborne datasets from multiple locations to assess global atmospheric changes, it will become increasingly important to ensure comparability of data quality, a process that has begun through the grounding of a World Calibration Center for VOCs, although this dataset predates this initiative.”

3.2 Overview of IAGOS-CARIBC observations

In total 6,607 Northern Hemispheric samples were collected during Feb 2006-Feb 2016. 51% of them (3,365 samples) are identified as upper tropospheric samples ($PV < 2$ PVU), the rest 49% (3,242) samples are stratospheric samples (Figure 1). All samples are categorized into four groups based on their sampling locations: North America (NAM), Asia (ASI), Europe (EUR), and Rest of the world (ROW) (Figure 1, Table S1). Temporal and spatial distributions of sample numbers are shown in Figure S2.

The observed upper tropospheric ethane ~~concentration~~mole fraction shows clear seasonality (Figure ~~24~~) driven by the atmospheric hydroxyl radical (OH) cycle and emissions. Upper tropospheric NAM and EUR ethane ~~concentration~~mole fractions increase from October/November peaking in April, decreases from April until October. This is consistent with the FTIR observation (Franco et al., 2015). Upper tropospheric ASI ethane peaks in June, two months later than NAM and EUR, and has two smaller peaks in October and February. Ethane mole fraction shows a stronger and different seasonality in EUR compared to the other regions. One possible explanation for this is relatively less a weaker influence by the in-mixing of stratospheric air over EUR. In contrast, the stratospheric ethane ~~concentration~~mole fractions does not show strong any clear seasonality, except that NAM has a seasonal trend with 3-month later shift compared to the upper tropospheric NAM trend, and stratospheric ASI ethane shows the same timing peak in June with upper tropospheric ASI ethane which potentially indicates the intrusion of tropospheric air masses into the stratosphere due to Asian summer monsoon (Xiong et al., 2009; Park et al., 2007). There is little seasonality evident in the ethane mole fractions in the stratosphere. Since stratospheric aircraft measurement campaigns are generally of short duration (several weeks), a direct comparison to previous data is not possible, however, vertical column data obtained by ground based FTIR for 8-21km reported by Helmig et al. (2016) also showed no clear seasonal variation.

3.3 Tropospheric trends

290 3.3.1 Upper tropospheric observation vs. model simulation

~~Figure 2 shows~~The upper tropospheric ethane trends (Figure 3) and corresponding uncertainties (Figure S3 (a)) from the observations, the model and model optimizations (section 2.2), the top 5 contributing model sectors, and the climatology are shown in Figures 3, S3 and section 2.2, correspondingly.

295 As the air samples were not collected in exactly the same positions (e.g. altitude, latitude, longitude), the observed trends of trace gases could be potentially influenced by biases between the sampling locations. ~~The trends presented in this study represent those from a selected number of observations.~~ In order to assess whether a sampling location bias is associated with the derived trend, the measured trends were compared to results from a global model (EMAC) where the

300 modeled data were extracted at the nearest grid of latitude, longitude, altitude, and time to the original measurement. Figure 32 (a) (grey line) shows the upper tropospheric ethane trend from the EMAC simulation with constant meteorology and constant year-to-year emission with seasonal cycle (climatology). Thus if a trend is indicated from the model data, then it is expected to be associated with the sampling location rather than a real underlying trend. Although small variations
305 of the ethane trend are observed due to the sampling location, these are negligible compared to the trend derived from the observations, implying that the different spatio-temporal sampling locations did not influence the estimated trends.

We then focus on the ethane trends in the whole NH upper troposphere, and in addition, three regions: NAM, EUR, and ASI, whose emissions are estimated to be the dominant sources of global
310 ethane emissions, accounting for 58--63% in 2008 (Monks et al., 2018). A clear increasing trend in ethane between Feb 2006-May 2010 of 19.2%/yr (± 4.8 , 1SD) relative to Feb 2006 and a decreasing trend in May 2010-Feb 2016 of 7.5%/yr (± 1.1) relative to May 2010 were observed for the upper troposphere (Figure 32 (a)). Such trend patterns are observed for all three regions of interest (NAM, ASI, EUR in Figure 32 (b)(c)(d)). Interestingly they are the inverse of the trends
315 observed at the surface stations: a decreasing trend before 2009 and a sharp increase in 2009-2014 (Simpson et al., 2012; Franco et al., 2015; Franco et al., 2016; Helmig et al., 2016). To understand the driving factors behind the observed trends, we simulated the ethane ~~concentration~~ mole fractions with the atmospheric model (EMAC) for the IAGOS-CARIBIC samples (see section 2.2).

The trends from the model simulations and the optimized model results (increasing the input model
320 emissions by 45%) are shown in Figure 32 as red and blue lines. The initial model results underestimate ethane ~~concentration~~ mole fractions by about 45%, whereas the model estimation is closer to observation ~~performance is much better with the same model and observation dataset~~ for ~~the simulation of~~ methane with the same model and observation dataset (Zimmermann et al., 2020). The model incorporates all known emissions via emission inventories so any deviations between
325 model and measurements can be interpreted as indicators of hitherto unknown emissions or sinks, atmospheric processes, or errors in emission inventories. The optimized model results match reasonably well with the measured NH upper tropospheric trend (Figure 32 (a)). However, this is not the case for the regional scales. A significant discrepancy between model and observation for NAM and ASI appears in 2010-2011 (Figure 32 (b)(c)). As the model includes fixed emissions or

330 emissions with prescribed changes, such an abrupt increase in the ethane trend for NAM and ASI
in 2010-2011 is presumably due to a short-term additional source that generated a large-scale
ethane plume. ~~A likely source is the Deepwater Horizon oil spill in 2010 that released 0.64 billion
liters oil into the Gulf of Mexico followed by a global transport of ethane to other continents
(Camilli et al., 2010; Unified Command Deepwater Horizon, 2010; Ryerson et al., 2011).~~ The
335 model simulates an inverse trend compared to the observed trend for EUR (Figure 32 (d)), although
the CAMS-GLOB-ANT dataset has already included emission inventories for some major
European cities (Guevara et al., 2021).

The top 5 contributing model sectors for ethane source trends are FEF (fugitives), RES (residential
energy use), TRO (road transportation), SWD (solid waste and waste water), and BIB (biomass
340 burning), and their optimized trends are shown in Figure 32. Interestingly the FEF opt contribution
is comparable to RES opt, which highlights the importance of fugitive emissions to the global
ethane budget as has been previously noted by Helmig et al. (2016). The pronounced peak in 2010-
2011 for the modeled NH upper tropospheric ethane is related to the increase in FEF, RES, and
SWD, and the decreasing trend in 2011-2013 can be explained by the decrease in FEF, RES, and
345 BIB (Figure 32 (a)). SWD and TRO contributed most ~~for to~~ the trends in NAM, ASI, and EUR,
while FEF, BIB, and RES have similar contribution (Figure 32 (b)(c)(d)). -We note that TRO, SWD,
and other sectors listed in Table 1 are modeled results.

Figure S43 shows the modeled sectoral contribution to regional and global ethane trends. The width
of flow is proportional to the quantity of sectoral contribution. Our model results estimated the
350 average contribution of biogenic (BIO), biomass burning (BIB), and anthropogenic sources (sum
of all other sectors) to the NH upper tropospheric ethane in 2006-2016 are 9%, 16%, and 75%,
respectively. This matches the estimated ~4%, 18%, and 78%, respectively, from Helmig et al.
(2016). The contribution of the top anthropogenic sources to upper tropospheric ethane are TRO
(28.7%), SWD (21.7%), FEF (14.0%), RES (6.0%), AWB (1.7%), and ENE (1.1%). Detailed
355 relative contributions of each sector are shown in Table S2. The contribution of TRO from this
study is more than that of ~10% estimated by Warneke et al. (2012); Peischl et al. (2013); Wunch
et al. (2016).

3.3.2 Model geographical sector contribution

360 ~~Five-Four~~ geographical sectors, i.e. ASI, NAM, EUR, and ROW ~~and AIR+BIB+BIO (as they~~
~~cannot be separated into regions)~~, were included to investigate the origin of the ethane emissions
(Figure 4, Figure S54). Geographical sectors refer to the regions where the emissions came from,
whereas “geographical regions” (Table S1) refer to the locations where the aircraft samples were
collected. Ethane emission from ASI dominates the trends for the whole NH upper troposphere,
365 NAM, ASI, and EUR, contributing ~~30%–55%, 35%–50%, 50%–65%, and 30%–40%, 35%–60%,~~
~~40%–60%, 60%–70%, and 37%–47%, respectively for 2006–2016.~~ Ethane emissions from ROW
~~and AIR+BIB+BIO~~ contribute ~~150%–4025% each~~ to the overall ethane trends in the upper
troposphere. Emissions from EUR and NAM are the least contributors with each only 5%–~~250%~~
contribution to ethane trends. Large contributions of ethane emissions from ASI to other regions
370 indicated that our air samples collected at ~10 km were originated from a large spatial scale, and
thus the observed ethane trends should not be interpreted as local emissions.

3.3.3 Upper tropospheric ~~E~~ethane, methane, and propane trend comparison

Methane and propane share emission sources with ethane, including fossil fuel extraction, transport,
375 and use, especially related to oil and natural gas (Helmig et al., 2016; Dalsøren et al., 2018;
Bourtsoukidis et al., 2020; Zimmermann et al., 2020). Further, these three compounds share the
same major sink in the atmosphere: oxidation by OH radical.

In 2006–2016, NH upper tropospheric ethane has a total change of 18.1 (mean) [min, max: -27.2,
29.4] ppt from observation, that corresponds to a ~~change rate~~ linear trend (described in section 2.3)
380 of ~~1.84~~ [-2.7, 2.9] ppt/yr, and 0.33 [-0.45, 0.55]%/yr relative to 2006. The observed NH upper
tropospheric methane increases in total 63.2 [62.7, 63.6] ppb, corresponding to a ~~growth rate~~ linear
trend of ~~6.32~~ [6.3, 6.4] ppb/yr (~~3.52~~ [3.549, 3.655] %/yr relative to 2006). In the same period, the
observed NH upper tropospheric propane increases in total 7.0 [-7.3, 11.1] ppt, representing a
~~growth rate~~ linear trend of 0.70 [-0.73, 1.11] ppt/yr (1.02 [-0.82, 1.72]%/yr relative to 2006). Zhang
385 et al. (2011) presented a ~3 %/yr increase of upper tropospheric methane at 206 hPa over China
from 2006–2008 using satellite observations, which matches the methane trend from our study.

For the whole NH upper troposphere, ethane and propane have similar trends in 2006-2016 (i.e. a rise and then a fall), whilst the observed methane trend follows an increase throughout that period (Figure 5). A common peak of all three compounds appears in 2010-2011, which possibly indicates an abrupt increase in oil and gas emissions. This peak is also observed for ASI, EUR, ROW and NAM (not for NAM methane) (Figures ~~S5, S6, S7~~S6, S7, S8, S9), suggesting regional and global increase in fossil fuel emissions. The contribution of OH radical variation to the peak in 2010-2011 is expected to be small as several previous studies have shown the atmospheric OH concentration did not change significantly in that period (Rigby et al., 2017; Li et al., 2018; Ipcc, 2013; Montzka et al., 2011). NAM ethane and propane trends from the middle of 2014 to 2016 show a clear decline, probably due to a slowdown in U.S. natural gas emissions (Angot et al., 2021).

~~3.3.4 Model simulation for ground stations~~

~~Observations of surface ethane mixing ratios at two ground stations (Mauna Loa (MLO), and Hohenpeissenberg (HPB)) were compared with model simulations using the optimized emissions from this study. The model predicts the ethane at the surface well, for both stations in NAM and EUR. This confirms that the optimized ethane emission budget derived from the upper tropospheric and stratospheric observation is realistic for surface-level ethane too.~~

~~3.3.5~~3.3.4 Ethane emission estimationbudget

~~Observations of surface ethane mixing ratios at two ground stations (Mauna Loa (MLO), and Hohenpeissenberg (HPB)) were compared with model simulations using the optimized emissions from this study (Figure S10). It is noted that the good agreement between two ground station observations and model simulations does not grant the accuracy of our model, further model results for ground level ethane should be studied in the future.~~

The global ethane emission ~~budget~~ was estimated to be 19.~~328~~328 Tg/yr for February 2006 to February 2016, with biogenic emissions 0.~~878~~878 Tg/yr, biomass burning 1.~~546~~546 Tg/yr, and anthropogenic emissions 17.~~105~~105 Tg/yr (Table 1). This ~~estimation~~estimation ~~budget~~ matches well with the estimated ethane

415 emissions from other studies, e.g. 18.2 Tg/yr for 2014 from Franco et al. (2016) and somewhat higher than the 15.3 Tg/yr (anthropogenic emission) for 2014 from Pozzer et al. (2020).

3.4 Stratospheric trends

3.4.1 Observation vs. model simulation

420 While ground based stations will be affected by upwind sources, the stratospheric samples offer a remote and averaged global perspective. Stratospheric ethane trends, estimated with all the IAGOS-CARIBIC samples taken in the NH lowermost stratosphere with ~~potential velocity (PV)~~ larger than 2 PVU during 2006-2016, along with modeled stratospheric trends, are shown in Figure 6 (corresponding uncertainties in Figure S3 (b)). The variation of the stratospheric climatology (Figure 6 (a)) indicates the sampling location bias for the observed stratospheric ethane trend. It varies more than the tropospheric one (Figure 3), but it is again a minor contribution ~~for observed trends~~, so that location biased trends can be discounted. The observed stratospheric ethane over the whole NH shows a general trend of -3.6 (± 0.3)/yr in 2006-2016, with two exceptional peaks in 2010 and 2013. The peak in 2010 is not seen at regional levels (NAM, ASI, EUR, Figure 6 (b)(c)(d)), which suggests would have indicated global upward transport of the upper tropospheric ethane ~~emissions~~ (peaking in 2010-2011) into the stratosphere and the important contribution from ROW. ~~The second peak in 2013 can is assumed to~~ be due to the regional emission transport into the lowermost stratosphere as such a peak is observed simultaneously over NAM and ASI. In general, the optimized model trend matches well with the observed NH stratospheric trend in 2006-435 2013 (Figure 6 (a)). A noticeable discrepancy between the optimized model simulation and observation appears since 2013. In the stratosphere, the OH radical concentration on average decreases by a factor of 10 compared with tropospheric OH levels, whereas Cl radicals are more abundant and therefore plays a greater relative role in ethane oxidation (Li et al., 2018). The loss of ethane in the stratosphere by reaction with Cl radicals is about 40 times more than that by OH radicals (reaction rate of ethane with Cl is about 400 times faster than with OH at 250K (Atkinson et al., 2001), and stratospheric OH is about ten times more abundant than stratospheric Cl (Li et al., 2018)), whereas the ethane loss in the troposphere by Cl is negligible compared with by OH due to the small amounts of tropospheric Cl (OH:Cl around 10,000) (Lelieveld et al., 1999; Gromov et

al., 2018)). The chlorine chemistry is not included in our model but the abundance of chlorine in
445 the stratosphere is a significant loss factor for ethane, thus part of the observed discrepancy can
come from the missing chlorine chemistry in the model. After 2013, the model prediction for ASI
was far from observation (Figure 6(c)), but this was not the case for other regions. Previous studies
have shown that the global and Asian emissions of some chlorinated trace gases (e.g. CFC-11,
CHCl₃) were increasing during 2012-2016 (Rigby et al., 2019; Fang et al., 2019; Montzka et al.,
450 2021), and strong chlorine chemistry was associated with Asian outflow in the UTLS region in
2013 (Baker et al., 2016). This could ~~also be an explain~~an explanation for the larger discrepancy
between model and observation since 2013 in ASI.

The top 5 contributing model sectors for stratospheric ethane trends, at global and regional scales,
are TRO (~28%), SWD (~24%), BIB (~15%), FEF (~13%), and RES (7%) (Figure 3, Table S2),
455 their optimized trends are shown in Figure 6.

Model geographical sector contributions for the stratospheric ethane trends are shown in Figure 7
and Figure S811. Similar to the upper troposphere, ASI ethane emissions contribute the most to the
global and regional stratospheric ethane trends (~5045%). We attribute this to the Asian Monsoon
transport of air pollutants from the troposphere to the stratosphere, which is supported by other
460 studies (Lelieveld et al., 2018; Randel et al., 2010; Park et al., 2009; Lelieveld et al., 2002; Bian et
al., 2020). Ethane emissions from ROW ~~and AIR+BIB+BIO~~ contributes 2015-250%-each, and
EUR and NAM 10-2015% each.

3.4.2 Stratospheric Ethane, methane, and propane trend comparison

465 Figure 8 shows the observed stratospheric trends of ethane, methane, and propane in 2006-2016.
The observed NH stratospheric ethane has a total change of -191.3 [-221.2, -166.7] ppt
corresponding to a ~~change rate~~linear trend of -19.13 [-22.12, -16.767] ppt/yr, and -3.6 [-4.15,
3.20] %/yr relative to 2006. The observed methane in the NH stratosphere increases in total 36.9
[34.5, 38.0] ppb, that represents a ~~growth rate~~linear trend of 3.769 [3.45, 3.80] ppb/yr (2.109
470 [2.01-95, 2.215] %/yr) relative to 2006. In the same period, the observed NH stratospheric propane
declined in total 52.2 [51.3, 55.7] ppt, that corresponds to a ~~decline rate~~linear trend of -5.22 [-5.6,
-5.13, -5.57] ppt/yr (-5.658 [-6.1, -5.545, -6.09] %/yr) relative to 2006. Rohs et al. (2006) derived
an increase in stratospheric methane (~30km) of ~5 %/yr using balloon-born observations for

475 1978-2003, and Rinsland et al. (2009) presented a larger increase (~8 %/yr) for the lower stratosphere in 1985-2008. The regional trends of ethane, propane, and methane at NAM, ASI, and EUR and ROW are shown in Figures S12-9, S10, and S11-S15.

Similar to the upper tropospheric trends, ethane and propane shared similar trends in the NH stratosphere, NAM, and EUR. The 2010-2011 peak observed in the upper troposphere also appears in the stratosphere, indicating a strong influence of troposphere-stratosphere exchange. It is noted
480 that the observed stratospheric trends on regional scales represent a mixture of local emission and global atmospheric transport.

3.5 Limitations and implications

485

Despite the usefulness, uniqueness and high quality of our datasets, several limitations of our study should be noted. (a) representativeness of the presented trends. Although our flight sampling is frequent and covers a large area of the NH, the spatial and temporal distributions of our samples are not even. This may cause the trends being influenced by a specific regions where more samples were collected. (b) chlorine chemistry is missing in the EMAC model. Chlorine radicals are much more abundant in the stratosphere than the surface, thus the change in chlorine plays a great role in the observed trends. (c) our samples were collected in the UTLS region and can be influenced by atmospheric transport (e.g. troposphere-stratosphere exchange), surface sources, and chemical destruction processes. Therefore, the trends represent the net effects of these factors making the interpretation on a single factor difficult. (d) PV choice of identifying upper tropospheric and stratospheric samples. In this study, we used PV=2 to define the tropopause, whereas other approaches exist. It is shown that on large space and time scales in the extratropics, the WMO tropopause corresponds rather well to a surface of constant potential vorticity (PV), although there exist systematic differences on smaller scales (Stohl et al., 2003; Wirth, 2000). (e) trend analysis tool “Prophet”. One needs some experience with the algorithm to choose and tune some parameters to get the best results for individual datasets, i.e. settings for

490
495
500

our dataset may not be suitable for other datasets. (f) model optimization. Our EMAC model and input values for sectorial emissions have been examined and optimized in many previous studies, therefore, in this study we simply increased each emission sector by 45% to match the observations. The aim of model simulations is to better understand the contributions from each emission sector, rather than improving the performance of model and emission inventories. (g) interpretation of results. This article is designed as a data description article to provide high quality and useful dataset for scientific use. There are many interesting features in the presented trends to be explored, however, it is beyond the aim of this study.

Implications. (a) observations of ethane, methane and propane were often restricted at regional scale or short-duration. We have presented a long-term (10 years) airborne observations of ethane, methane and propane in the UTLS region at northern hemispheric scale. This dataset is unique and can be used to examine long-term troposphere-stratosphere exchange, chemical and dynamical changes in the UTLS region, and improve model performance. To the best of our knowledge, such long-term aircraft observations are only available from IAGOS-CARIBIC project (our study) and CONTRAIL project (Machida et al., 2008; Sawa et al., 2015). (b) The “Prophet” algorithm is an open source software, and suitable for non-continuous time-series datasets. Unlike the commonly used linear fit approach for trend analysis in other studies, the “Prophet” algorithm is robust to missing data and the influence from outliers is minimized. It better captures the inter-annual variability and is not influenced by the time period of choice. (c) other analysis approaches such as machine learning techniques can be used on our dataset to enlarge the spatial and temporal distributions. Combining our dataset with space-borne observations will provide a better view of global distributions and trends of trace gases.

3 Data availability

The NOAA ethane ground station data can be downloaded from NOAA website (<https://gml.noaa.gov/>). The IAGOS-CARIBIC observational data of ethane, methane, and propane in the period February 2006 – February 2016, and optimized ethane mixing ratios in sectors from EMAC model simulation for the same IAGOS-CARIBIC samples and time period, can be accessed at <https://doi.org/10.5281/zenodo.54420596301729> (Li et al., 2021). Co-authorship may be appropriate if the IAGOS-CARIBIC data are essential for a result or conclusion of a publication.

4 Conclusions

In this study, we present upper tropospheric and lower stratospheric ethane trends from airborne observations and atmospheric modeling over the period 2006-2016. The model performance was optimized by scaling to the observational data. We identified ethane sectoral sources to which observed average trends over ten years (2006-2016) and three continents (North America, Europe, and Asia) could be attributed from observation and modeling. Trends of ethane, propane, and methane from observation were compared to identify ethane emission sources. The major findings are summarized as follows:

- The global ethane emission budget for February 2006 to February 2016 was estimated to be 19.328 Tg/yr. In the Northern Hemisphere, the upper tropospheric ethane had an increasing trend of $0.33 \pm 0.27\%/yr$ and the stratospheric ethane had a decreasing trend of $-3.6 \pm 0.3\%/yr$ for 2006-2016. The current inventory [from CAMS-GLOB-ANT v4.2](#) underestimates ethane emission by roughly a factor of three.
- The top five contributing model sectors for upper tropospheric and stratospheric ethane trends are FEF (fugitives), RES (residential energy use), TRO (road transportation), SWD (solid waste and waste water), and BIB (biomass burning). Emissions from Asia dominate the observed ethane trends for both upper troposphere and lower stratosphere.
- A sharp increase in the observed upper tropospheric and stratospheric ethane trends at global and regional scales in 2010-2011 was caused by fossil fuel related emissions, likely from oil associated and natural gas sources. In contrast to methane, the global ethane trends cannot be well simulated by advanced atmospheric chemistry modeling, which suggests the need of accurate and frequent observations of global ethane and the improvement of emission inventories.

Author contribution

M.L. and J.W. developed the idea of this study. M.L. wrote the first draft of the manuscript. A.P. run the model simulations. All authors contributed to discussing and revising the manuscript.

Competing interests

The authors declare no conflict of interests.

Acknowledgement

565 We are thankful to Sourangsu Chowdhury for preparing the model emission input data into different regions, and Nils Noll for providing biomass burning emission budget for ethane. We thank Tobias Sattler for contributing to the initial idea of this study. We thank NOAA for sharing ground station data of ethane. We thank Python, Esri and Figdraw for providing statistical and plotting tools. We thank the editor Nellie Elguindi and three anonymous reviewers.

570

References

- Angelbratt, J., Mellqvist, J., Simpson, D., Jonson, J. E., Blumenstock, T., Borsdorff, T., Duchatelet, P., Forster, F., Hase, F., Mahieu, E., De Mazière, M., Notholt, J., Petersen, A. K., Raffalski, U., Servais, C., Sussmann, R., Warneke, T., and Vigouroux, C.: Carbon monoxide (CO) and ethane (C₂H₆) trends from ground-based solar FTIR measurements at six European stations, comparison and sensitivity analysis with the EMEP model, *Atmos. Chem. Phys.*, 11, 9253-9269, 10.5194/acp-11-9253-2011, 2011.
- 575
- Angot, H., Davel, C., Wiedinmyer, C., Pétron, G., Chopra, J., Hueber, J., Blanchard, B., Bourgeois, I., Vimont, I., Montzka, S. A., Miller, B. R., Elkins, J. W., and Helmig, D.: Temporary pause in the growth of atmospheric ethane and propane in 2015–2018, *Atmos. Chem. Phys.*, 2021, 1-34, 10.5194/acp-2021-285, 2021.
- 580
- Atkinson, R., Baulch, D., Cox, R., Crowley, J., Hampson Jr, R., Kerr, J., Rossi, M., and Troe, J.: Summary of evaluated kinetic and photochemical data for atmospheric chemistry, IUPAC Subcommittee on gas kinetic data evaluation for atmospheric chemistry, 20, 2001.
- 585
- Baker, A. K., Slemr, F., and Brenninkmeijer, C. A. M.: Analysis of non-methane hydrocarbons in air samples collected aboard the CARIBIC passenger aircraft, *Atmos. Meas. Tech.*, 3, 311-321, 10.5194/amt-3-311-2010, 2010.
- Baker, A. K., Sauvage, C., Thorenz, U. R., van Velthoven, P., Oram, D. E., Zahn, A., Brenninkmeijer, C. A., and Williams, J.: Evidence for strong, widespread chlorine radical
- 590

- chemistry associated with pollution outflow from continental Asia, *Scientific reports*, 6, 1-9, 2016.
- 595 Bian, J., Li, D., Bai, Z., Li, Q., Lyu, D., and Zhou, X.: Transport of Asian surface pollutants to the global stratosphere from the Tibetan Plateau region during the Asian summer monsoon, *National Science Review*, 7, 516-533, 2020.
- 600 Bourtsoukidis, E., Pozzer, A., Sattler, T., Matthaios, V. N., Ernle, L., Edtbauer, A., Fischer, H., Könemann, T., Osipov, S., Paris, J. D., Pfannerstill, E. Y., Stöner, C., Tadic, I., Walter, D., Wang, N., Lelieveld, J., and Williams, J.: The Red Sea Deep Water is a potent source of atmospheric ethane and propane, *Nature Communications*, 11, 447, 10.1038/s41467-020-14375-0, 2020.
- 605 Brenninkmeijer, C. A. M., Crutzen, P., Boumard, F., Dauer, T., Dix, B., Ebinghaus, R., Filippi, D., Fischer, H., Franke, H., Frieß, U., Heintzenberg, J., Helleis, F., Hermann, M., Kock, H. H., Koepfel, C., Lelieveld, J., Leuenberger, M., Martinsson, B. G., Miemczyk, S., Moret, H. P., Nguyen, H. N., Nyfeler, P., Oram, D., O'Sullivan, D., Penkett, S., Platt, U., Pupek, M., Ramonet, M., Randa, B., Reichelt, M., Rhee, T. S., Rohwer, J., Rosenfeld, K., Scharffe, D., Schlager, H., Schumann, U., Slemr, F., Sprung, D., Stock, P., Thaler, R., Valentino, F., van Velthoven, P., Waibel, A., Wandel, A., Waschitschek, K., Wiedensohler, A., Xueref-Remy, I., Zahn, A., Zech, U., and Ziereis, H.: Civil Aircraft for the regular investigation of the atmosphere based on an instrumented container: The new CARIBIC system, *Atmos. Chem. Phys.*, 7, 4953-4976, 610 10.5194/acp-7-4953-2007, 2007.
- Camilli, R., Reddy, C. M., Yoerger, D. R., Van Mooy, B. A. S., Jakuba, M. V., Kinsey, J. C., McIntyre, C. P., Sylva, S. P., and Maloney, J. V.: Tracking Hydrocarbon Plume Transport and Biodegradation at Deepwater Horizon, *Science*, 330, 201, 10.1126/science.1195223, 2010.
- 615 Dalsøren, S. B., Myhre, G., Hodnebrog, Ø., Myhre, C. L., Stohl, A., Pisso, I., Schwietzke, S., Höglund-Isaksson, L., Helmig, D., Reimann, S., Sauvage, S., Schmidbauer, N., Read, K. A., Carpenter, L. J., Lewis, A. C., Punjabi, S., and Wallasch, M.: Discrepancy between simulated and observed ethane and propane levels explained by underestimated fossil emissions, *Nature Geoscience*, 11, 178-184, 10.1038/s41561-018-0073-0, 2018.
- 620 Emmons, L. K., Arnold, S. R., Monks, S. A., Huijnen, V., Tilmes, S., Law, K. S., Thomas, J. L., Raut, J. C., Bouarar, I., Turquety, S., Long, Y., Duncan, B., Steenrod, S., Strode, S., Flemming, J., Mao, J., Langner, J., Thompson, A. M., Tarasick, D., Apel, E. C., Blake, D. R., Cohen, R. C., Dibb, J., Diskin, G. S., Fried, A., Hall, S. R., Huey, L. G., Weinheimer, A. J., Wisthaler, A., Mikoviny, T., Nowak, J., Peischl, J., Roberts, J. M., Ryerson, T., Warneke, C., and Helmig, D.: The POLARCAT Model Intercomparison Project (POLMIP): overview and evaluation with 625 observations, *Atmos. Chem. Phys.*, 15, 6721-6744, 10.5194/acp-15-6721-2015, 2015.
- Fang, X., Park, S., Saito, T., Tunnicliffe, R., Ganesan, A. L., Rigby, M., Li, S., Yokouchi, Y., Fraser, P. J., and Harth, C. M.: Rapid increase in ozone-depleting chloroform emissions from China, *Nature Geoscience*, 12, 89-93, 2019.
- 630 Fischer, E. V., Jacob, D. J., Yantosca, R. M., Sulprizio, M. P., Millet, D. B., Mao, J., Paulot, F., Singh, H. B., Roiger, A., Ries, L., Talbot, R. W., Dzepina, K., and Pandey Deolal, S.: Atmospheric peroxyacetyl nitrate (PAN): a global budget and source attribution, *Atmos. Chem. Phys.*, 14, 2679-2698, 10.5194/acp-14-2679-2014, 2014.

- 635 Franco, B., Bader, W., Toon, G. C., Bray, C., Perrin, A., Fischer, E. V., Sudo, K., Boone, C. D., Bovy, B., Lejeune, B., Servais, C., and Mahieu, E.: Retrieval of ethane from ground-based FTIR solar spectra using improved spectroscopy: Recent burden increase above Jungfraujoch, *Journal of Quantitative Spectroscopy and Radiative Transfer*, 160, 36-49, 10.1016/j.jqsrt.2015.03.017, 2015.
- 640 Franco, B., Mahieu, E., Emmons, L. K., Tzompa-Sosa, Z. A., Fischer, E. V., Sudo, K., Bovy, B., Conway, S., Griffin, D., Hannigan, J. W., Strong, K., and Walker, K. A.: Evaluating ethane and methane emissions associated with the development of oil and natural gas extraction in North America, *Environmental Research Letters*, 11, 044010, 10.1088/1748-9326/11/4/044010, 2016.
- 645 Gardiner, T., Forbes, A., de Mazière, M., Vigouroux, C., Mahieu, E., Demoulin, P., Velazco, V., Notholt, J., Blumenstock, T., Hase, F., Kramer, I., Sussmann, R., Stremme, W., Mellqvist, J., Strandberg, A., Ellingsen, K., and Gauss, M.: Trend analysis of greenhouse gases over Europe measured by a network of ground-based remote FTIR instruments, *Atmos. Chem. Phys.*, 8, 6719-6727, 10.5194/acp-8-6719-2008, 2008.
- 650 González Abad, G., Allen, N. D. C., Bernath, P. F., Boone, C. D., McLeod, S. D., Manney, G. L., Toon, G. C., Carouge, C., Wang, Y., Wu, S., Barkley, M. P., Palmer, P. I., Xiao, Y., and Fu, T. M.: Ethane, ethyne and carbon monoxide concentrations in the upper troposphere and lower stratosphere from ACE and GEOS-Chem: a comparison study, *Atmospheric Chemistry and Physics*, 11, 9927-9941, 10.5194/acp-11-9927-2011, 2011.
- 655 Granier, C., Darras, S., van der Gon, H. D., Jana, D., Elguindi, N., Bo, G., Michael, G., Marc, G., Jalkanen, J.-P., and Kuenen, J.: The Copernicus Atmosphere Monitoring Service global and regional emissions (April 2019 version), 2019.
- 660 Gromov, S., Brenninkmeijer, C. A., and Jöckel, P.: A very limited role of tropospheric chlorine as a sink of the greenhouse gas methane, *Atmospheric Chemistry and Physics*, 18, 9831-9843, 2018.
- 665 Guevara, M., Jorba, O., Tena, C., Denier van der Gon, H., Kuenen, J., Elguindi-Solmon, N., Darras, S., Granier, C., and Pérez García-Pando, C.: CAMS-TEMPO: global and European emission temporal profile maps for atmospheric chemistry modelling, *Earth Syst. Sci. Data*, 2021, 1-60, 10.5194/essd-2020-175, 2020.
- 670 Guevara, M., Jorba, O., Tena, C., Denier van der Gon, H., Kuenen, J., Elguindi, N., Darras, S., Granier, C., and Pérez García-Pando, C.: Copernicus Atmosphere Monitoring Service TEMPO profiles (CAMS-TEMPO): global and European emission temporal profile maps for atmospheric chemistry modelling, *Earth Syst. Sci. Data*, 13, 367-404, 10.5194/essd-13-367-2021, 2021.
- 675 Harvey, A. C. and Shephard, N.: 10 Structural time series models, 1993.
- Hausmann, P., Sussmann, R., and Smale, D.: Contribution of oil and natural gas production to renewed increase in atmospheric methane (2007–2014): top–down estimate from ethane and methane column observations, *Atmos. Chem. Phys.*, 16, 3227-3244, 10.5194/acp-16-3227-2016, 2016.
- Helmig, D., Rossabi, S., Hueber, J., Tans, P., Montzka, S. A., Masarie, K., Thoning, K., Plass-Duelmer, C., Claude, A., Carpenter, L. J., Lewis, A. C., Punjabi, S., Reimann, S., Vollmer, M. K., Steinbrecher, R., Hannigan, J. W., Emmons, L. K., Mahieu, E., Franco, B., Smale, D., and Pozzer, A.: Reversal of global atmospheric ethane and propane trends largely due to US oil and natural gas production, *Nature Geoscience*, 9, 490-495, 10.1038/ngeo2721, 2016.

- Hersbach, H., Bell, B., Berrisford, P., Hirahara, S., Horányi, A., Muñoz-Sabater, J., Nicolas, J., Peubey, C., Radu, R., Schepers, D., Simmons, A., Soci, C., Abdalla, S., Abellan, X., Balsamo, G., Bechtold, P., Biavati, G., Bidlot, J., Bonavita, M., De Chiara, G., Dahlgren, P., Dee, D., Diamantakis, M., Dragani, R., Flemming, J., Forbes, R., Fuentes, M., Geer, A., Haimberger, L., 680 Healy, S., Hogan, R. J., Hólm, E., Janisková, M., Keeley, S., Laloyaux, P., Lopez, P., Lupu, C., Radnoti, G., de Rosnay, P., Rozum, I., Vamborg, F., Villaume, S., and Thépaut, J.-N.: The ERA5 global reanalysis, *Quarterly Journal of the Royal Meteorological Society*, 146, 1999-2049, <https://doi.org/10.1002/qj.3803>, 2020.
- IPCC: Climate change 2013: the physical science basis: Working Group I contribution to the 685 Fifth assessment report of the Intergovernmental Panel on Climate Change, edited by: Stocker, T. F., Qin, D., Plattner, G.-K., Tignor, M., Allen, S. K., Boschung, J., Nauels, A., Xia, Y., Bex, V., and Midgley, P. M., Cambridge university press 2013.
- Jöckel, P., Kerkweg, A., Pozzer, A., Sander, R., Tost, H., Riede, H., Baumgaertner, A., Gromov, S., and Kern, B.: Development cycle 2 of the Modular Earth Submodel System (MESSy2), 690 *Geosci. Model Dev.*, 3, 717-752, 10.5194/gmd-3-717-2010, 2010.
- Karu, E., Li, M., Ernle, L., Brenninkmeijer, C. A., Lelieveld, J., and Williams, J.: Atomic emission detector with gas chromatographic separation and cryogenic pre-concentration (CryoTrap-GC-AED) for trace gas measurement, *Atmospheric Measurement Techniques*, 10.5194/amt-2020-199, 2021.
- 695 Kort, E. A., Smith, M. L., Murray, L. T., Gvakharia, A., Brandt, A. R., Peischl, J., Ryerson, T. B., Sweeney, C., and Travis, K.: Fugitive emissions from the Bakken shale illustrate role of shale production in global ethane shift, *Geophysical Research Letters*, 43, 4617-4623, <https://doi.org/10.1002/2016GL068703>, 2016.
- Lelieveld, J., Bregman, A., Scheeren, H., Ström, J., Carslaw, K., Fischer, H., Siegmund, P., and 700 Arnold, F.: Chlorine activation and ozone destruction in the northern lowermost stratosphere, *Journal of Geophysical Research: Atmospheres*, 104, 8201-8213, 1999.
- Lelieveld, J., Berresheim, H., Borrmann, S., Crutzen, P., Dentener, F., Fischer, H., Feichter, J., Flatau, P., Heland, J., and Holzinger, R.: Global air pollution crossroads over the Mediterranean, *Science*, 298, 794-799, 2002.
- 705 Lelieveld, J., Bourtsoukidis, E., Brühl, C., Fischer, H., Fuchs, H., Harder, H., Hofzumahaus, A., Holland, F., Marno, D., and Neumaier, M.: The South Asian monsoon—pollution pump and purifier, *Science*, 361, 270-273, 2018.
- Li, M., Pozzer, A., Lelieveld, J., and Williams, J.: [Northern hemispheric atmospheric ethane trends \(2006-2016\) with reference to methane and propane](#)~~Global atmospheric ethane, propane and methane trends (2006-2016)~~ [data set] [dataset], 10.5281/zenodo.51120596301729, 2021. 710
- Li, M., Karu, E., Ciais, P., Lelieveld, J., and Williams, J.: The empirically determined integrated atmospheric residence time of carbon dioxide (CO₂), in review, 2022.
- Li, M., Karu, E., Brenninkmeijer, C., Fischer, H., Lelieveld, J., and Williams, J.: Tropospheric OH and stratospheric OH and Cl concentrations determined from CH₄, CH₃Cl, and SF₆ 715 measurements, *Nature Climate and Atmospheric Science*, 1, 10.1038/s41612-018-0041-9, 2018.
- Machida, T., Matsueda, H., Sawa, Y., Nakagawa, Y., Hirokuni, K., Kondo, N., Goto, K., Nakazawa, T., Ishikawa, K., and Ogawa, T.: Worldwide measurements of atmospheric CO₂ and

- other trace gas species using commercial airlines, *Journal of Atmospheric and Oceanic Technology*, 25, 1744-1754, 2008.
- 720 Millet, D. B., Guenther, A., Siegel, D. A., Nelson, N. B., Singh, H. B., de Gouw, J. A., Warneke, C., Williams, J., Eerdekens, G., Sinha, V., Karl, T., Flocke, F., Apel, E., Riemer, D. D., Palmer, P. I., and Barkley, M.: Global atmospheric budget of acetaldehyde: 3-D model analysis and constraints from in-situ and satellite observations, *Atmos. Chem. Phys.*, 10, 3405-3425, 10.5194/acp-10-3405-2010, 2010.
- 725 Monks, S. A., Wilson, C., Emmons, L. K., Hannigan, J. W., Helmig, D., Blake, N. J., and Blake, D. R.: Using an Inverse Model to Reconcile Differences in Simulated and Observed Global Ethane Concentrations and Trends Between 2008 and 2014, *Journal of Geophysical Research: Atmospheres*, 123, 11,262-211,282, <https://doi.org/10.1029/2017JD028112>, 2018.
- 730 Montzka, S. A., Krol, M., Dlugokencky, E., Hall, B., Jockel, P., and Lelieveld, J.: Small interannual variability of global atmospheric hydroxyl, *Science*, 331, 67-69, 10.1126/science.1197640, 2011.
- Montzka, S. A., Dutton, G. S., Portmann, R. W., Chipperfield, M. P., Davis, S., Feng, W., Manning, A. J., Ray, E., Rigby, M., and Hall, B. D.: A decline in global CFC-11 emissions during 2018– 2019, *Nature*, 590, 428-432, 2021.
- 735 Park, M., Randel, W. J., Emmons, L. K., and Livesey, N. J.: Transport pathways of carbon monoxide in the Asian summer monsoon diagnosed from Model of Ozone and Related Tracers (MOZART), *Journal of Geophysical Research: Atmospheres*, 114, 2009.
- 740 Park, M., Randel, W. J., Gettelman, A., Massie, S. T., and Jiang, J. H.: Transport above the Asian summer monsoon anticyclone inferred from Aura Microwave Limb Sounder tracers, *Journal of Geophysical Research: Atmospheres*, 112, 2007.
- 745 Peischl, J., Ryerson, T. B., Brioude, J., Aikin, K. C., Andrews, A. E., Atlas, E., Blake, D., Daube, B. C., de Gouw, J. A., Dlugokencky, E., Frost, G. J., Gentner, D. R., Gilman, J. B., Goldstein, A. H., Harley, R. A., Holloway, J. S., Kofler, J., Kuster, W. C., Lang, P. M., Novelli, P. C., Santoni, G. W., Trainer, M., Wofsy, S. C., and Parrish, D. D.: Quantifying sources of methane using light alkanes in the Los Angeles basin, California, *Journal of Geophysical Research: Atmospheres*, 118, 4974-4990, <https://doi.org/10.1002/jgrd.50413>, 2013.
- 750 Pétron, G., Karion, A., Sweeney, C., Miller, B. R., Montzka, S. A., Frost, G. J., Trainer, M., Tans, P., Andrews, A., Kofler, J., Helmig, D., Guenther, D., Dlugokencky, E., Lang, P., Newberger, T., Wolter, S., Hall, B., Novelli, P., Brewer, A., Conley, S., Hardesty, M., Banta, R., White, A., Noone, D., Wolfe, D., and Schnell, R.: A new look at methane and nonmethane hydrocarbon emissions from oil and natural gas operations in the Colorado Denver-Julesburg Basin, *Journal of Geophysical Research: Atmospheres*, 119, 6836-6852, <https://doi.org/10.1002/2013JD021272>, 2014.
- 755 Pozzer, A., Schultz, M. G., and Helmig, D.: Impact of U.S. Oil and Natural Gas Emission Increases on Surface Ozone Is Most Pronounced in the Central United States, *Environmental Science & Technology*, 54, 12423-12433, 10.1021/acs.est.9b06983, 2020.
- Randel, W. J., Park, M., Emmons, L., Kinnison, D., Bernath, P., Walker, K. A., Boone, C., and Pumphrey, H.: Asian monsoon transport of pollution to the stratosphere, *Science*, 328, 611-613, 2010.

- 760 Rigby, M., Park, S., Saito, T., Western, L., Redington, A., Fang, X., Henne, S., Manning, A., Prinn, R., and Dutton, G.: Increase in CFC-11 emissions from eastern China based on atmospheric observations, *Nature*, 569, 546-550, 2019.
- Rigby, M., Montzka, S. A., Prinn, R. G., White, J. W. C., Young, D., O'Doherty, S., Lunt, M. F., Ganesan, A. L., Manning, A. J., Simmonds, P. G., Salameh, P. K., Harth, C. M., Muhle, J.,
- 765 Weiss, R. F., Fraser, P. J., Steele, L. P., Krummel, P. B., McCulloch, A., and Park, S.: Role of atmospheric oxidation in recent methane growth, *Proc Natl Acad Sci U S A*, 114, 5373-5377, 10.1073/pnas.1616426114, 2017.
- Rinsland, C. P., Chiou, L., Boone, C., Bernath, P., Mahieu, E., and Zander, R.: Trend of lower stratospheric methane (CH₄) from atmospheric chemistry experiment (ACE) and atmospheric
- 770 trace molecule spectroscopy (ATMOS) measurements, *Journal of Quantitative Spectroscopy and Radiative Transfer*, 110, 1066-1071, 2009.
- Roeckner, E., Brokopf, R., Esch, M., Giorgetta, M., Hagemann, S., Kornblueh, L., Manzini, E., Schlese, U., and Schulzweida, U.: Sensitivity of Simulated Climate to Horizontal and Vertical Resolution in the ECHAM5 Atmosphere Model, *Journal of Climate*, 19, 3771-3791,
- 775 10.1175/JCLI3824.1, 2006.
- Rohs, S., Schiller, C., Riese, M., Engel, A., Schmidt, U., Wetter, T., Levin, I., Nakazawa, T., and Aoki, S.: Long - term changes of methane and hydrogen in the stratosphere in the period 1978–2003 and their impact on the abundance of stratospheric water vapor, *Journal of Geophysical Research: Atmospheres*, 111, 2006.
- 780 Rudolph, J.: The tropospheric distribution and budget of ethane, *Journal of Geophysical Research: Atmospheres*, 100, 11369-11381, 10.1029/95JD00693, 1995.
- Ryerson, T. B., Aikin, K. C., Angevine, W. M., Atlas, E. L., Blake, D. R., Brock, C. A., Fehsenfeld, F. C., Gao, R. S., de Gouw, J. A., Fahey, D. W., Holloway, J. S., Lack, D. A., Lueb, R. A., Meinardi, S., Middlebrook, A. M., Murphy, D. M., Neuman, J. A., Nowak, J. B., Parrish, D. D., Peischl, J., Perring, A. E., Pollack, I. B., Ravishankara, A. R., Roberts, J. M., Schwarz, J. P., Spackman, J. R., Stark, H., Warneke, C., and Watts, L. A.: Atmospheric emissions from the
- 785 Deepwater Horizon spill constrain air-water partitioning, hydrocarbon fate, and leak rate, *Geophysical Research Letters*, 38, <https://doi.org/10.1029/2011GL046726>, 2011.
- Sander, R., Jöckel, P., Kirner, O., Kunert, A. T., Landgraf, J., and Pozzer, A.: The photolysis module JVAL-14, compatible with the MESSy standard, and the JVal PreProcessor (JVPP), *Geosci. Model Dev.*, 7, 2653-2662, 10.5194/gmd-7-2653-2014, 2014.
- 790 Sawa, Y., Machida, T., Matsueda, H., Niwa, Y., Tsuboi, K., Murayama, S., Morimoto, S., and Aoki, S.: Seasonal changes of CO₂, CH₄, N₂O, and SF₆ in the upper troposphere/lower stratosphere over the Eurasian continent observed by commercial airliner, *Geophysical Research Letters*, 42, 2001-2008, 2015.
- 795 Schuck, T. J., Brenninkmeijer, C. A. M., Slemr, F., Xueref-Remy, I., and Zahn, A.: Greenhouse gas analysis of air samples collected onboard the CARIBIC passenger aircraft, *Atmos. Meas. Tech.*, 2, 449-464, 10.5194/amt-2-449-2009, 2009.
- Simpson, I. J., Sulbaek Andersen, M. P., Meinardi, S., Bruhwiler, L., Blake, N. J., Helmig, D.,
- 800 Rowland, F. S., and Blake, D. R.: Long-term decline of global atmospheric ethane concentrations and implications for methane, *Nature*, 488, 490-494, 10.1038/nature11342, 2012.

- Stohl, A., Bonasoni, P., Cristofanelli, P., Collins, W., Feichter, J., Frank, A., Forster, C., Gerasopoulos, E., Gäggeler, H., and James, P.: Stratosphere - troposphere exchange: A review, and what we have learned from STACCATO, *Journal of Geophysical Research: Atmospheres*, 108, 2003.
- Sun, Y., Yin, H., Liu, C., Mahieu, E., Notholt, J., Té, Y., Lu, X., Palm, M., Wang, W., Shan, C., Hu, Q., Qin, M., Tian, Y., and Zheng, B.: Reduction in C₂H₆ from 2015 to 2020 over Hefei, eastern China points to air quality improvement in China, *Atmos. Chem. Phys.*, 2021, 1-29, 10.5194/acp-2021-13, 2021.
- 805 Taylor, S. J. and Letham, B.: Forecasting at scale, *The American Statistician*, 72, 37-45, 2018.
- Tilmes, S., Lamarque, J. F., Emmons, L. K., Kinnison, D. E., Marsh, D., Garcia, R. R., Smith, A. K., Neely, R. R., Conley, A., Vitt, F., Val Martin, M., Tanimoto, H., Simpson, I., Blake, D. R., and Blake, N.: Representation of the Community Earth System Model (CESM1) CAM4-chem within the Chemistry-Climate Model Initiative (CCMI), *Geosci. Model Dev.*, 9, 1853-1890, 815 10.5194/gmd-9-1853-2016, 2016.
- Tzompa-Sosa, Z. A., Mahieu, E., Franco, B., Keller, C. A., Turner, A. J., Helmig, D., Fried, A., Richter, D., Weibring, P., Walega, J., Yacovitch, T. I., Herndon, S. C., Blake, D. R., Hase, F., Hannigan, J. W., Conway, S., Strong, K., Schneider, M., and Fischer, E. V.: Revisiting global fossil fuel and biofuel emissions of ethane, *Journal of Geophysical Research: Atmospheres*, 122, 820 2493-2512, <https://doi.org/10.1002/2016JD025767>, 2017.
- Unified Command Deepwater Horizon: US scientific teams refine estimates of oil flow from BP's well prior to capping, *Gulf of Mexico Oil Spill Response 2010*, 2010.
- Warneke, C., de Gouw, J. A., Holloway, J. S., Peischl, J., Ryerson, T. B., Atlas, E., Blake, D., Trainer, M., and Parrish, D. D.: Multiyear trends in volatile organic compounds in Los Angeles, 825 California: Five decades of decreasing emissions, *Journal of Geophysical Research: Atmospheres*, 117, <https://doi.org/10.1029/2012JD017899>, 2012.
- Wirth, V.: Thermal versus dynamical tropopause in upper - tropospheric balanced flow anomalies, *Quarterly Journal of the Royal Meteorological Society*, 126, 299-317, 2000.
- Wunch, D., Toon, G. C., Hedelius, J. K., Vizenor, N., Roehl, C. M., Saad, K. M., Blavier, J.-F. 830 L., Blake, D. R., and Wennberg, P. O.: Quantifying the loss of processed natural gas within California's South Coast Air Basin using long-term measurements of ethane and methane, *Atmospheric Chemistry and Physics*, 16, 14091-14105, 10.5194/acp-16-14091-2016, 2016.
- Xiao, Y., Logan, J. A., Jacob, D. J., Hudman, R. C., Yantosca, R., and Blake, D. R.: Global budget of ethane and regional constraints on U.S. sources, *Journal of Geophysical Research: 835 Atmospheres*, 113, 10.1029/2007JD009415, 2008.
- Xiong, X., Houweling, S., Wei, J., Maddy, E., Sun, F., and Barnet, C.: Methane plume over south Asia during the monsoon season: satellite observation and model simulation, *Atmospheric Chemistry and Physics*, 9, 783-794, 2009.
- Zhang, X., Bai, W., Zhang, P., and Wang, W.: Spatiotemporal variations in mid-upper 840 tropospheric methane over China from satellite observations, *Chinese Science Bulletin*, 56, 3321-3327, 2011.
- Zimmermann, P. H., Brenninkmeijer, C. A. M., Pozzer, A., Jöckel, P., Winterstein, F., Zahn, A., Houweling, S., and Lelieveld, J.: Model simulations of atmospheric methane (1997–2016) and

845 their evaluation using NOAA and AGAGE surface and IAGOS-CARIBIC aircraft observations,
Atmos. Chem. Phys., 20, 5787-5809, 10.5194/acp-20-5787-2020, 2020.

Figures and Tables

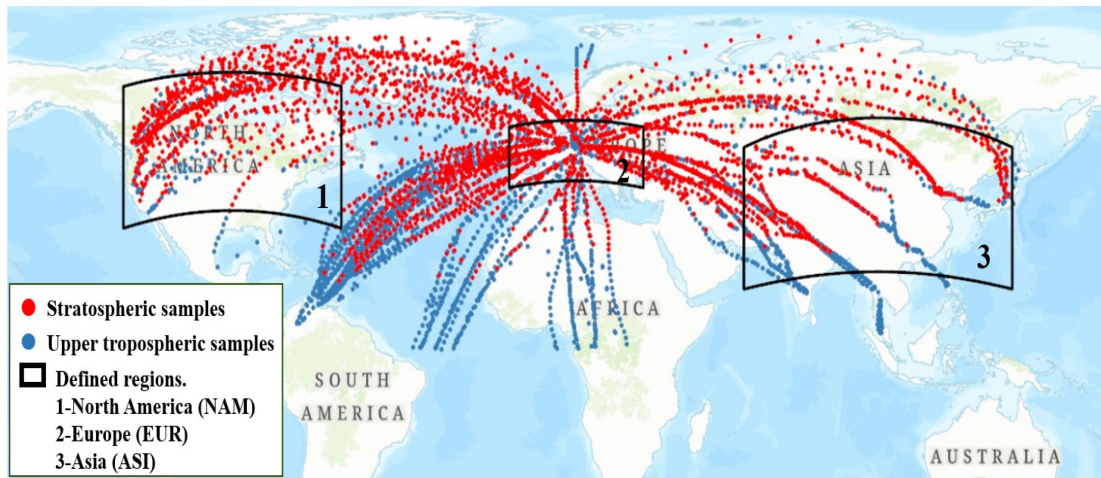
850

Table 1. Sectoral description and ethane emissions estimated from this study for Feb 2006-Feb 20016.

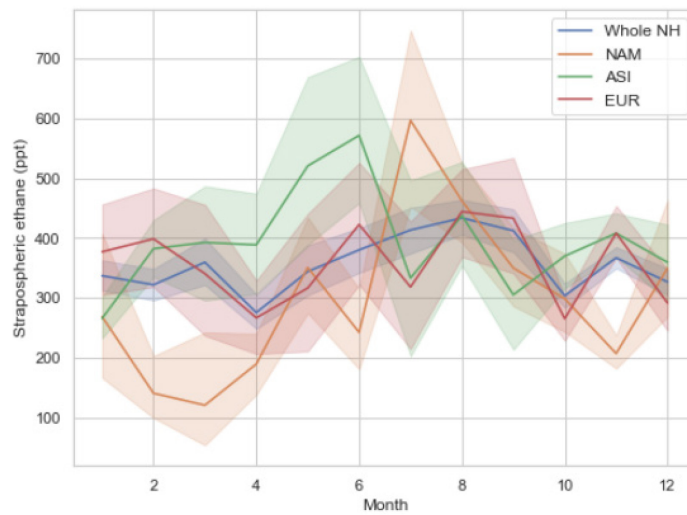
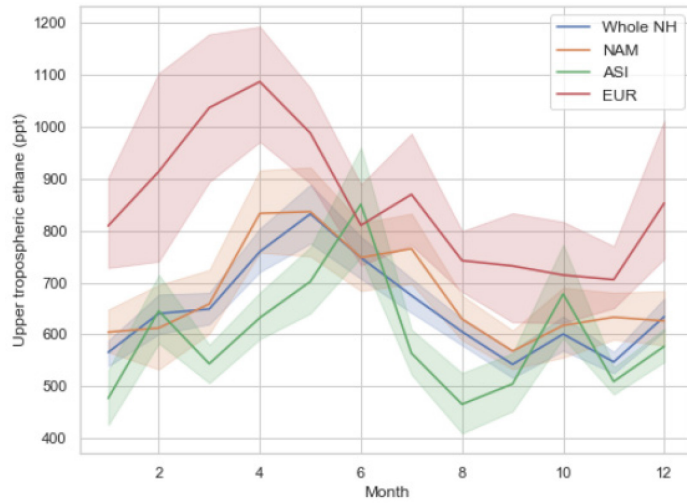
Sector	Description	<u>Emission from inventory (Tg/yr)</u>	<u>Estimated Emission (optimized)(Tg/yr)</u>
BIO	Biogenic emission	<u>0.54</u>	0.78
BIB	Biomass burning	<u>1.01</u>	1.46
(a) Anthropogenic by sector			
AWB	Agricultural waste burning	<u>0.08</u>	0.12
ENE	Power generation (power and heat plants, refineries, others)	<u>0.04</u>	0.06
FEF	Fugitives	<u>5.28</u>	7.65
IND	Industrial processes	<u>0.90</u>	1.30
RES	Residential energy use	<u>3.32</u>	4.82
SHP	Ships	<u>0.02</u>	0.03
SLV	Solvents	<u>0.00</u>	0.00
SWD	Solid waste and waste water	<u>1.01</u>	1.47
TNR	Off-road transportation	<u>0.01</u>	0.02
TRO	Road transportation	<u>1.10</u>	1.59
(b) Anthropogenic by geographical sector			
ASI	Emission from Asia	<u>5.16</u>	7.48
EUR	Emission from Europe	<u>1.60</u>	2.32
NAM	Emission from North America	<u>1.01</u>	1.46
ROW	Emission from rest of the world	<u>3.99</u>	5.79
Total source		<u>13.30</u>	19.28

855 Table 2. Summary of studies reporting ethane trends in the (a) troposphere and (b) stratosphere.

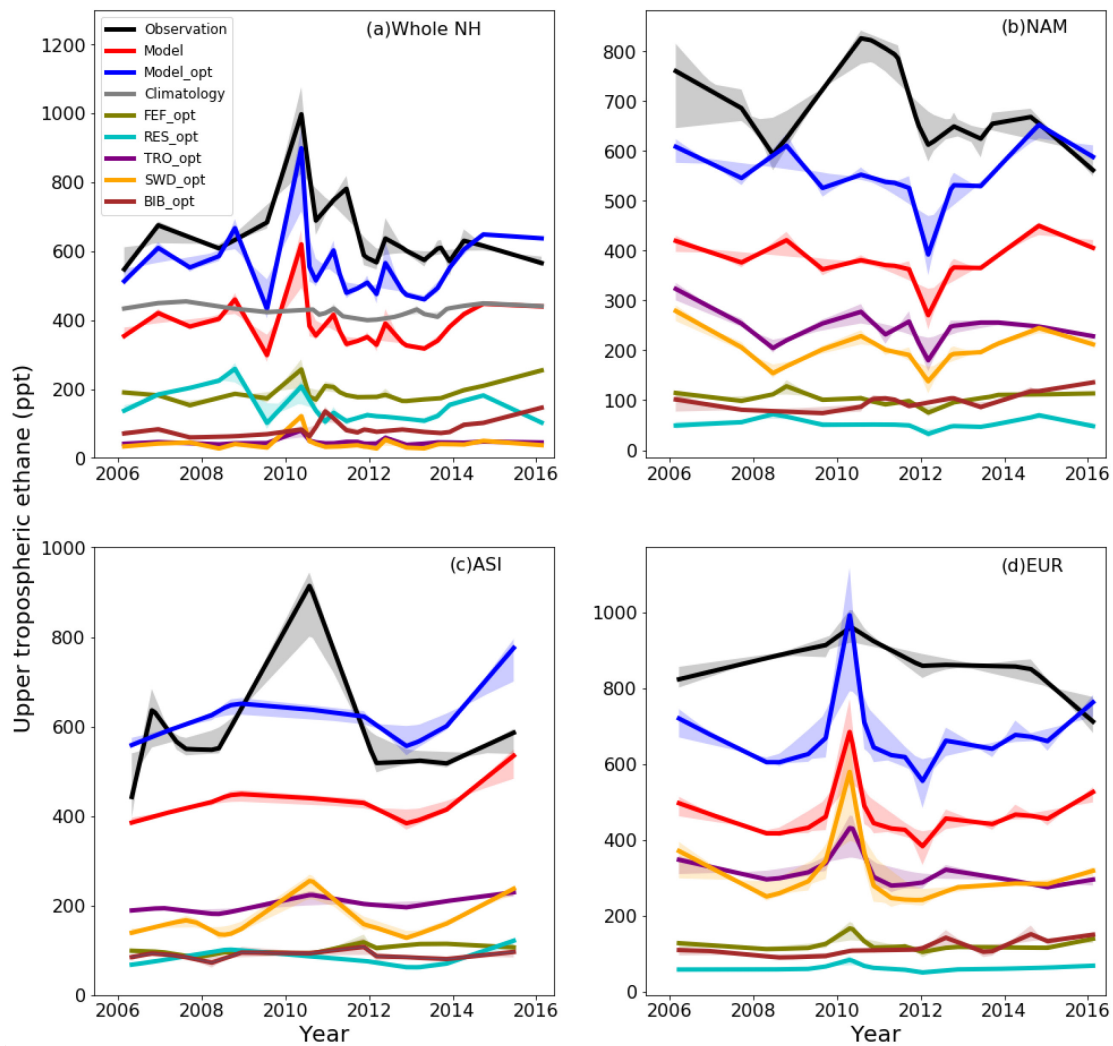
Trends (%/year)	Time period	References
(a) Tropospheric trends		
-1.09 ~ -2.11 (four European sites)	1996-2006	Angelbratt et al. (2011)
-0.81 (global)	1986-2010	Simpson et al. (2012)
-0.92 (Jungfraujoch, 47° N)	1994-2008	Franco et al. (2015)
4.9 (Jungfraujoch, 47° N)	2009-2014	Franco et al. (2015)
2.9-4.7 (32 ground sites)	2009-2014	Helmig et al. (2016)
3-5 (six sites)	2009-2014	Franco et al. (2016)
	compared with 2003-2008	
ca. 4.6 (Zugspitze, 47° N)	2007-2014	Hausmann et al. (2016)
ca. -2.5 (Lauder, 45° S)	2007-2014	Hausmann et al. (2016)
ca. 5.6 (GEOSummit, 73° N)	01.2010-12.2014	Angot et al. (2021)
-2.6 ± 1.34 (Hefei, 32° N)	2015-2020	Sun et al. (2021)
<u>-0.47 ~ -1.30 (mean: -1.13)</u>	<u>2007-2014</u>	<u>This study</u>
0.33 ± 0.27	02.2006-02.2016	This study
(Northern Hemispheric upper troposphere)		
(b) Stratospheric trends		
-3.31 ~ 0.43 (stratospheric column)	2000-2005	Gardiner et al. (2008)
-1.75 ± 1.30 (8-16km above Jungfraujoch)	2004-2008	Franco et al. (2015)
-1.0 ± 0.2 (8-21km above Jungfraujoch)	1995-2009	Helmig et al. (2016)
9.4 ± 3.2 (8-16km above Jungfraujoch)	2009-2013	Franco et al. (2015)
6.0 ± 1.1 (8-21km above Jungfraujoch)	2009-2015	Helmig et al. (2016)
-3.6 ± 0.3	02.2006-02.2016	This study
(Northern Hemispheric lowermost stratosphere)		

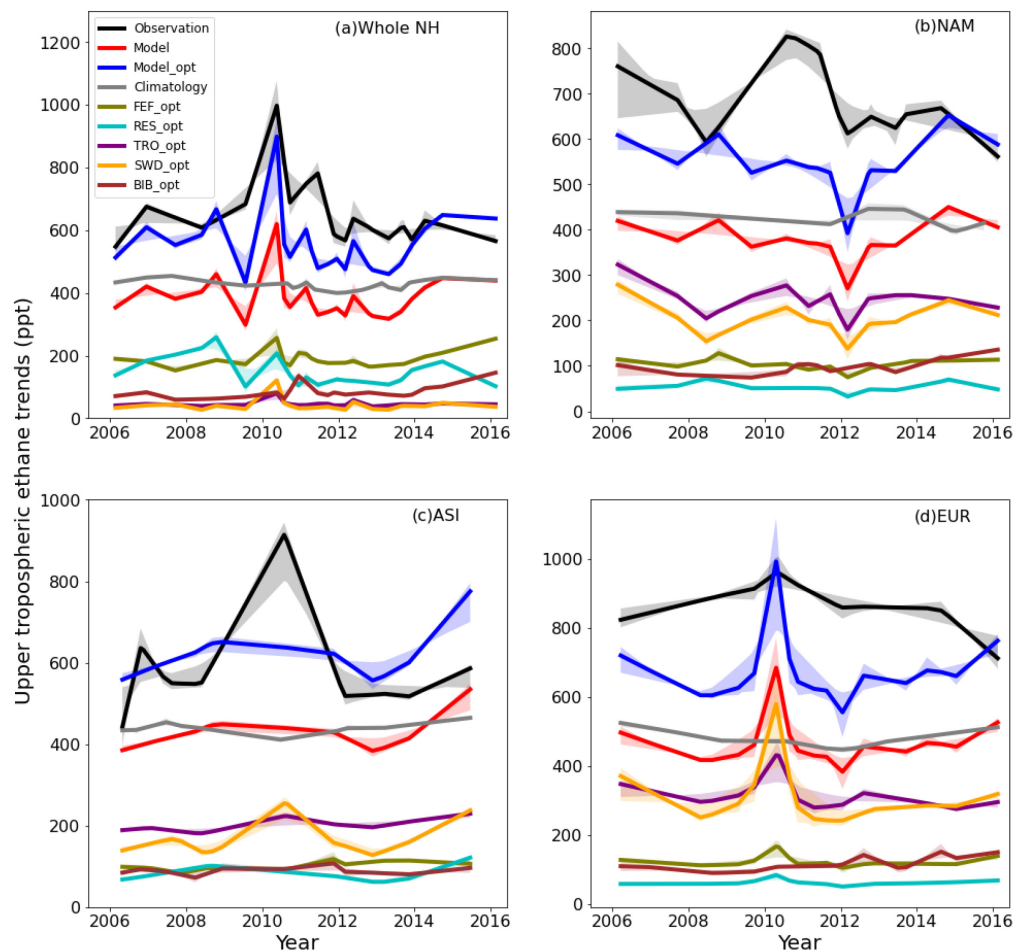


860 Figure 1. Geographical locations of aircraft samples (distinguished as upper tropospheric samples and stratospheric samples) and spatial segregation. Samples collected outside the black boxes are defined as ROW samples.



865 Figure 21. Seasonality of upper tropospheric and stratospheric ethane concentration mole fractions over the whole Northern Hemisphere (Whole NH), North America (NAM), Asia (ASI), and Europe (EUR).





875 Figure 32. Upper tropospheric ethane trends from observations, the model (Model: sum of all sectoral emissions) and model optimization (Model_opt: sum of all optimized sectoral emissions; sector abbreviation ends with “opt”: individual optimized sectoral emission), and climatology ~~and model optimization~~ for (a) the whole NH; (b) North America; (c) Asia; and (d) Europe. Light shadows indicate trend analysis uncertainty.

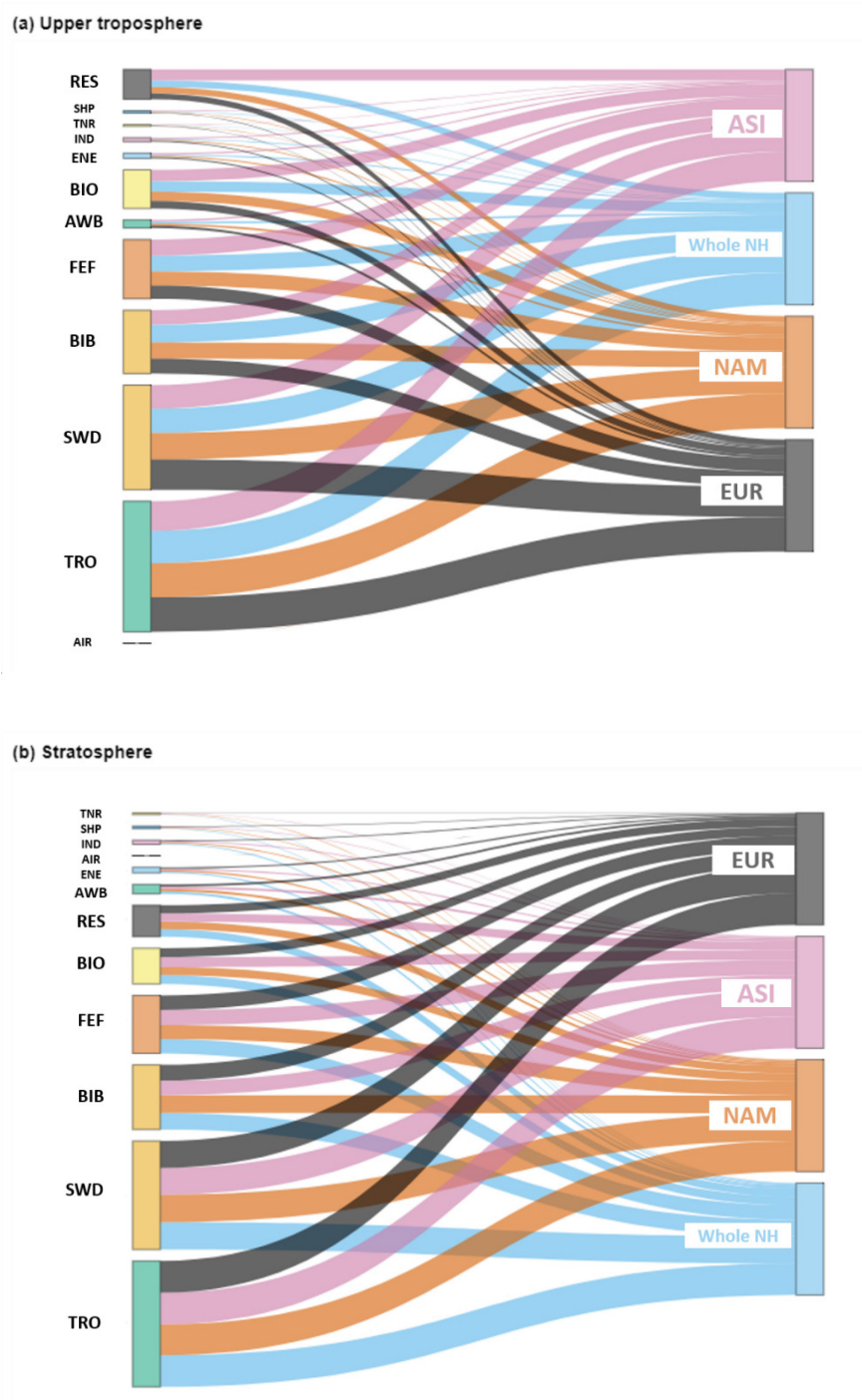
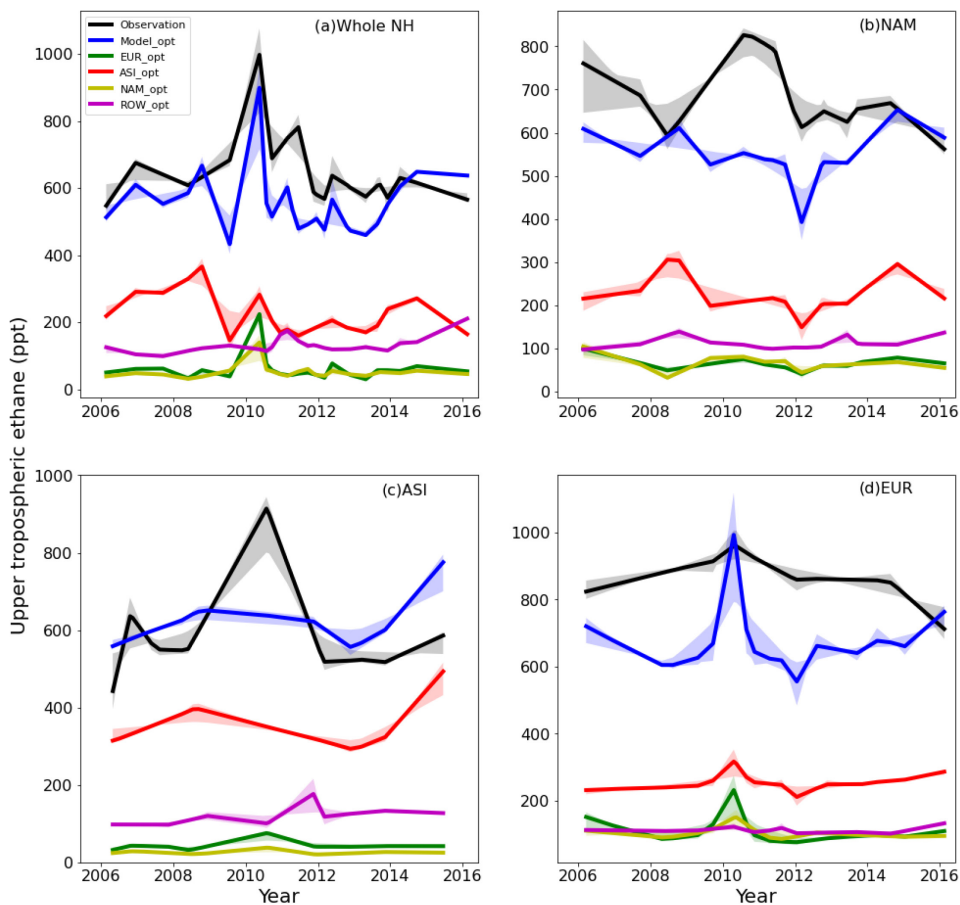
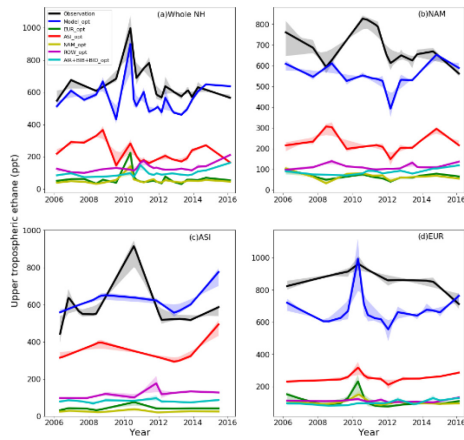


Figure 3. Sectoral contribution to ethane trends for the (a) upper troposphere and (b) stratosphere in 2006-2016.

885



890 Figure 4. Observed trends and modeled optimized (“opt”) geographical sector contribution (emissions originated from EUR, ASI, NAM, and ROW) to NH upper tropospheric ethane trends for (a) the whole NH; (b) North America; (c) Asia; and (d) Europe. Light shadows indicate trend analysis uncertainty. “Model_opt” indicates the sum of all optimized emission sectors.

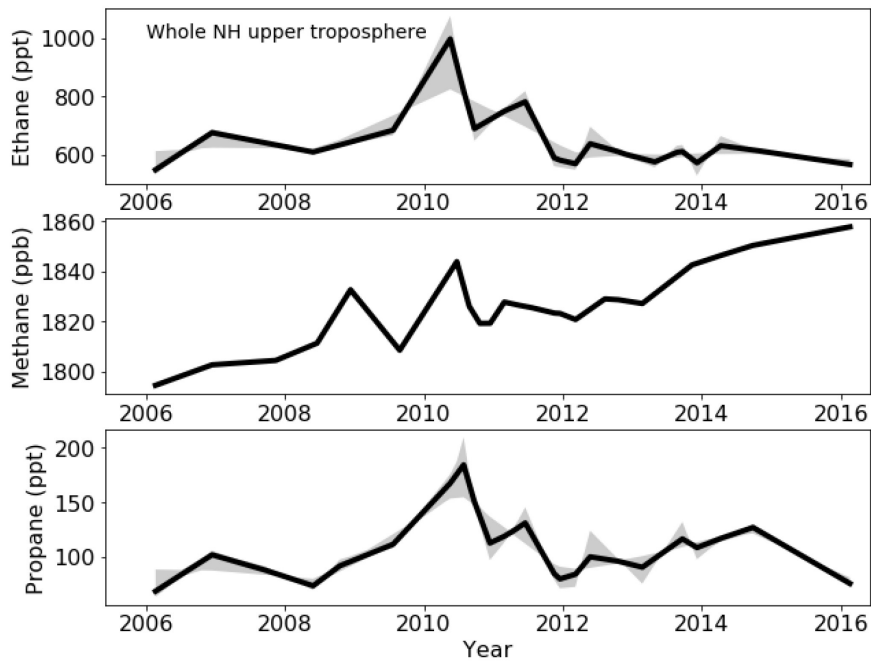
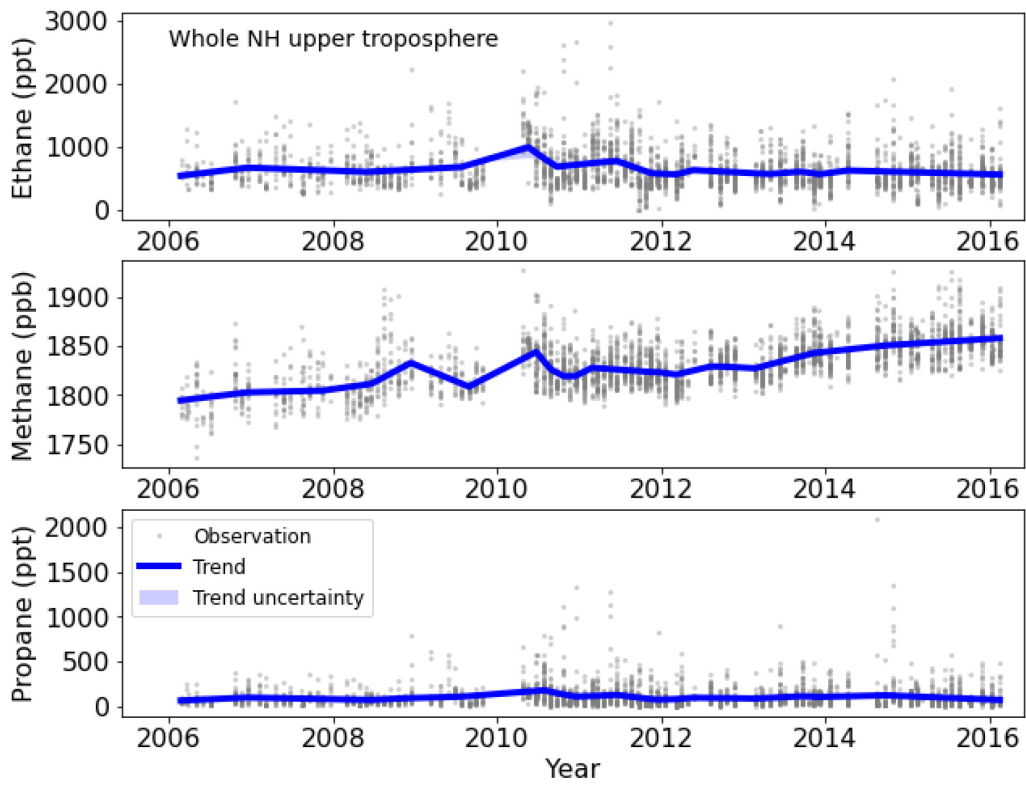
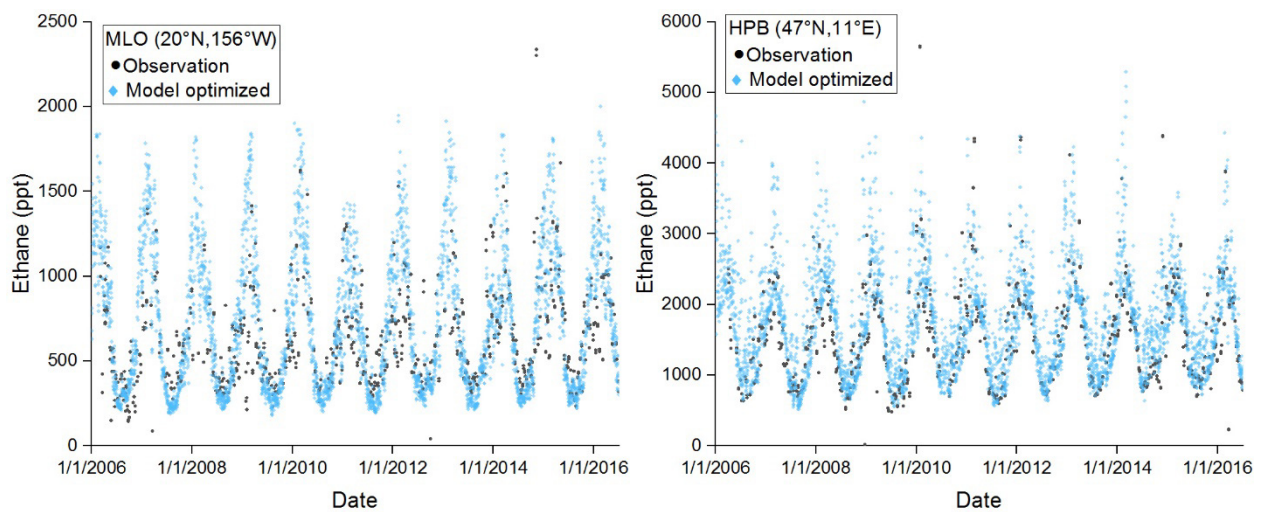


Figure 5. The observed (a)-ethane; (b), methane; (c) and propane mole fractions (gray dots) and trends (blue lines) for the whole NH upper troposphere. Light shadows indicate trend analysis uncertainty.

900



905 ~~Figure 5. Observations and optimized model simulations for ethane mixing ratios at two ground stations (MLO, HPB).~~

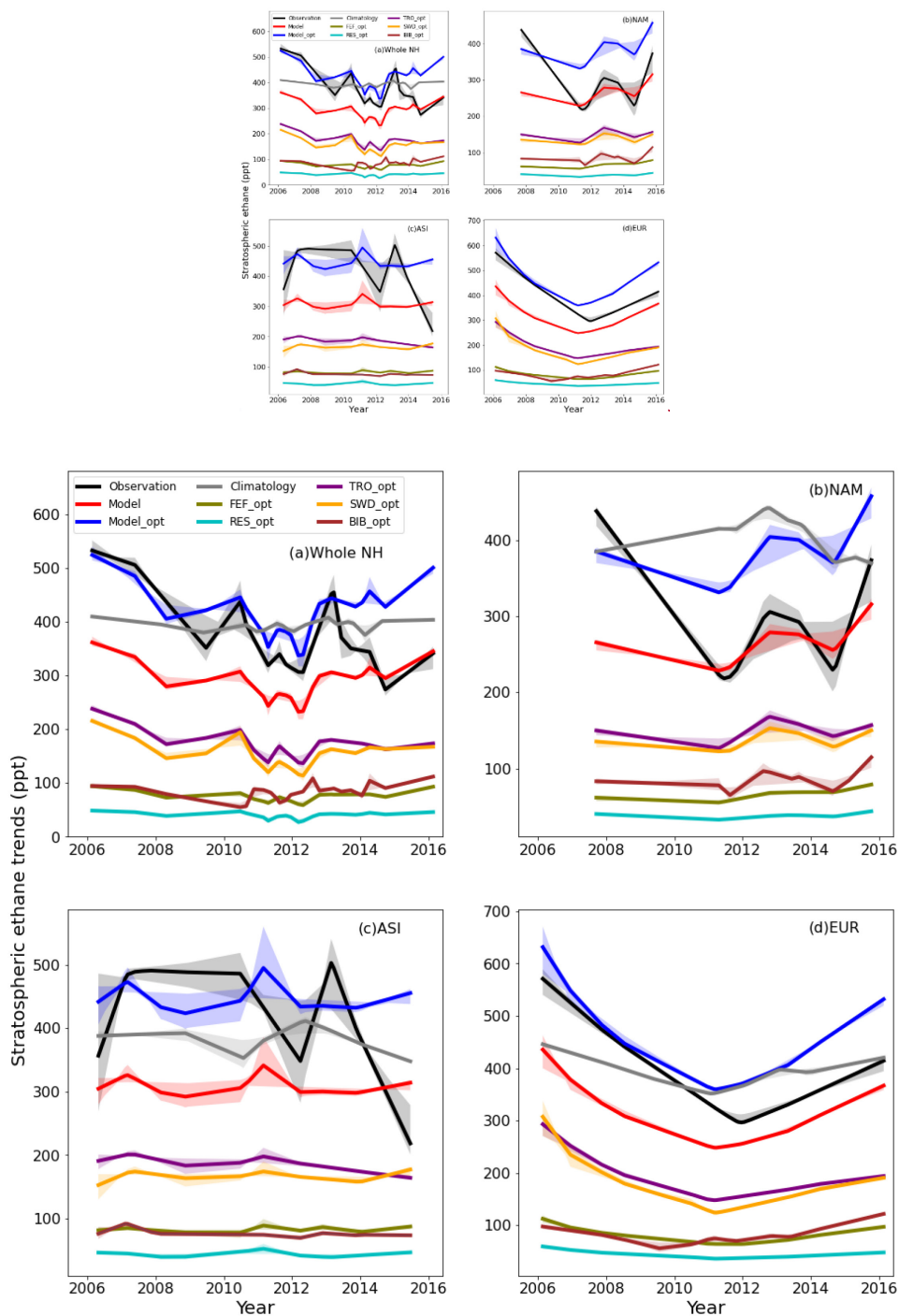
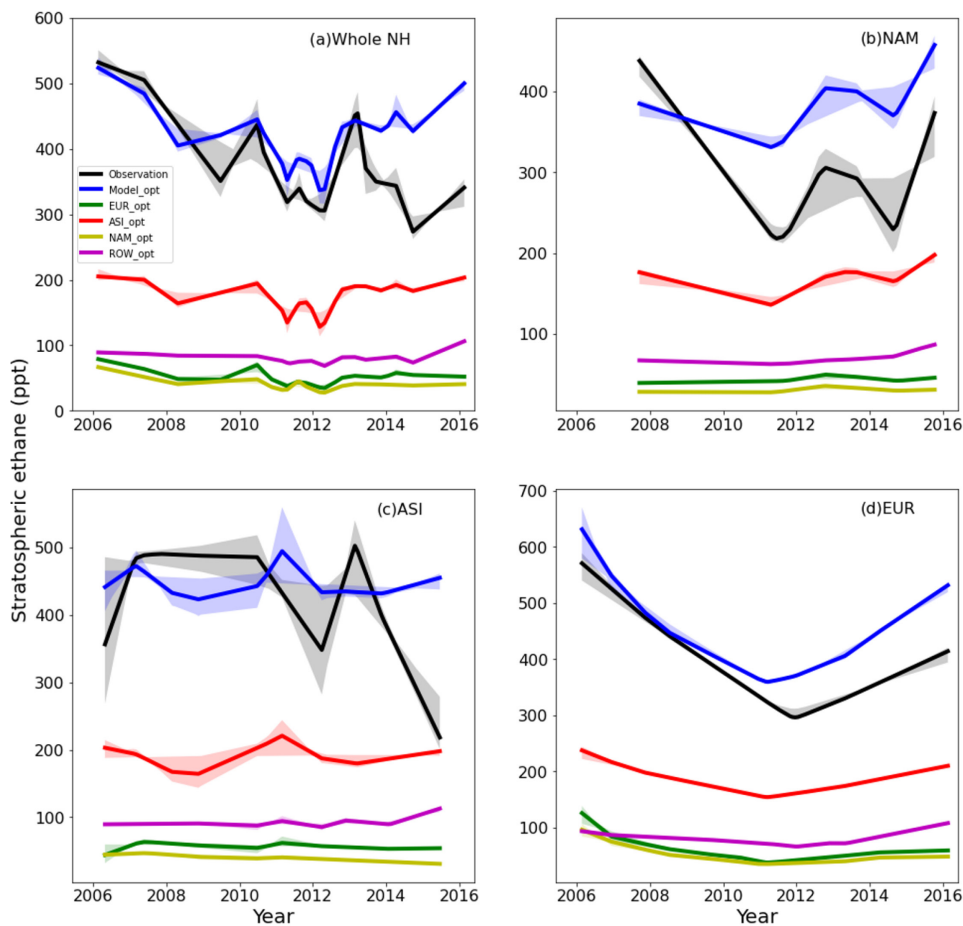
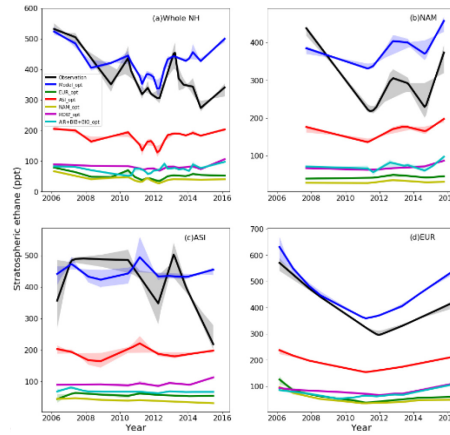


Figure 6. Stratospheric ethane trends from observation, model (Model: sum of all sectoral emissions) and model optimization (Model_opt: sum of all optimized sectoral emissions; sector

915 abbreviation ends with “opt”: individual optimized sectoral emission), and climatology and model optimization for (a) the whole NH stratosphere; (b) North America; (c) Asia; and (d) Europe. Light shadows indicate trend analysis uncertainty.



920 Figure 7. Observed trends and modeled optimized (“opt”) Optimized—geographical sector contribution (emissions originated from EUR, ASI, NAM, and ROW) to stratospheric ethane trends

for (a) the whole NH stratosphere; (b) North America; (c) Asia; and (d) Europe. Light shadows indicate trend analysis uncertainty. “Model_opt” indicates the sum of all optimized emission sectors.

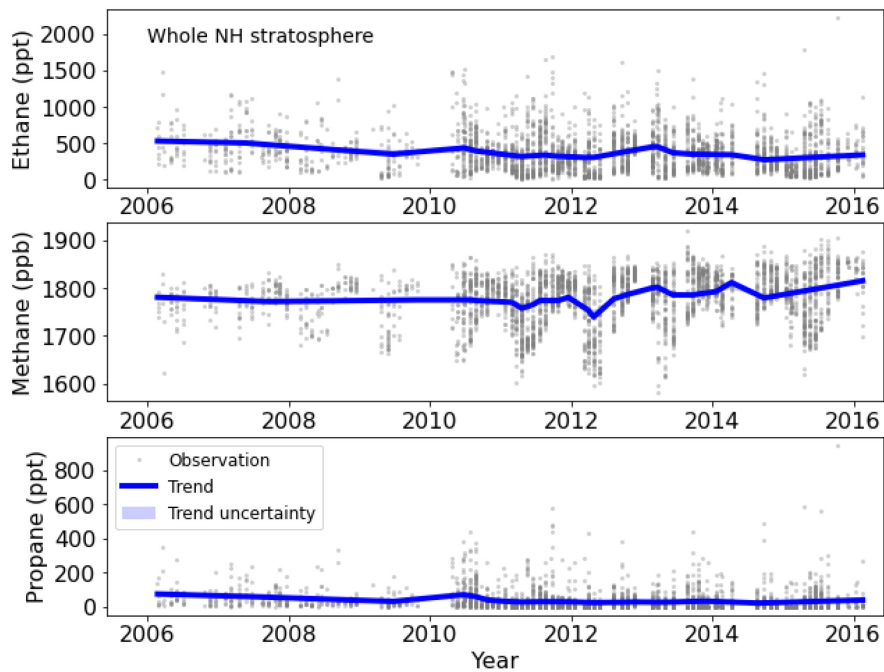
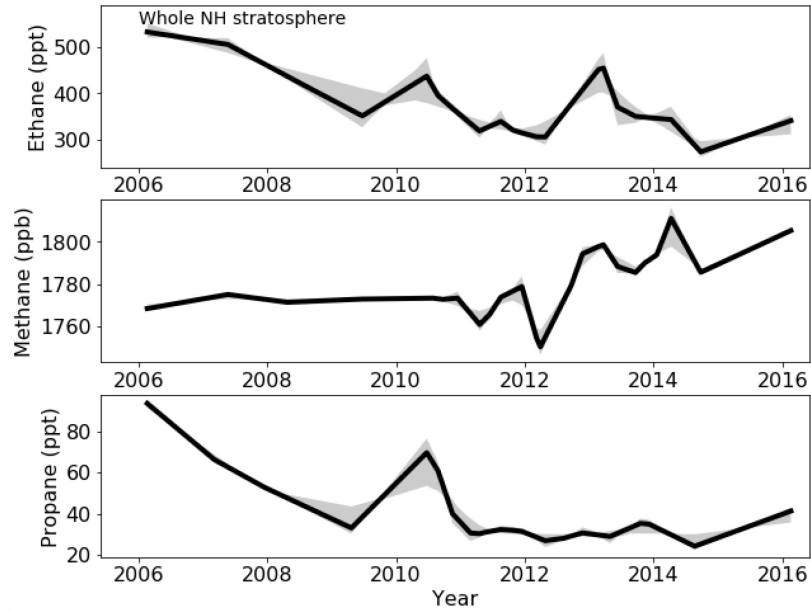


Figure 8. The observed (a) ethane, (b) methane, and (c) propane mole fractions (gray dots) and trends (blue lines) for the whole NH stratosphere. Light shadows indicate trend analysis uncertainty.

